Journal of Catalysis 306 (2013) 11–29

Contents lists available at SciVerse ScienceDirect

Journal of Catalysis

journal homepage: www.elsevier.com/locate/jcat

Formation of different promoted metallic phases in PtFe and PtSn catalysts supported on carbonaceous materials used for selective hydrogenation

Julieta P. Stassi *, Patricia D. Zgolicz, Sergio R. de Miguel, Osvaldo A. Scelza

Instituto de Investigaciones en Catálisis y Petroquímica (INCAPE), Facultad de Ingeniería Química, Universidad Nacional del Litoral – CONICET, Santiago del Estero 2654, 3000 Santa Fe, Argentina

ARTICLE INFO

Article history:
Received 22 March 2013
Revised 14 May 2013
Accepted 15 May 2013

Keywords:
Multi-wall carbon nanotubes
Carbon Vulcan XC-72
PtFe and PtSn catalysts
Support characterization
Metallic phase characterization
Citral selective hydrogenation

ABSTRACT

In this paper, a study on the selective hydrogenation of α,β-unsaturated aldehydes to unsaturated alcohols (UA) by using two series of PtSn and PtFe catalysts with different metallic loadings and supported on carbon nanotubes and carbon Vulcan is reported. The catalysts were prepared by conventional impregnation using the corresponding metallic precursors, H_2PtCl_6, $SnCl_2$, and $FeCl_3$. Once reduced under hydrogen flow, the supported catalysts were characterized by temperature-programmed reduction (TPR), H_2 chemisorption, test reactions of the metallic phase, and X-ray photoelectron spectroscopy (XPS). Hydrogenation results show that the addition of a second metal to Pt leads to important modification of the selectivity, although the highest selectivities to UA are reached with very different Fe or Sn loadings. The performance of the catalysts in the citral hydrogenation was related to the characteristics of the bimetallic phase. It was found that the Fe addition to Pt catalysts results in a typical behavior such as for an usual ionic promoter in contact with the active metal, reaching high selectivities to UA as the Fe loading and the Fe ionic species percentage increases, while for PtSn catalysts, a high selectivity to UA was found only with a very low amount of Sn ionic species in contact with a very high percentage of Sn reduced species. The best selectivity to UA (about 98%) was found for PtSn(1wt%)/CN-P catalyst treated with N_2 at high temperature.

1. Introduction

The use of carbonaceous materials as catalyst supports is continuously increasing due to they offer a greater versatility as compared to oxidic supports [1–3]. In general, carbon materials have been used for a long time in heterogeneous catalysis because they can satisfy most of the desirable properties required for a suitable support, such as good chemical stability, high thermal resistance in a non-oxidizing atmosphere, proper surface areas and porosity, good electronic properties, adequate mechanical properties, and easy recovery of precious metals [4,5]. The high flexibility in the selection of a specific carbon as catalytic support is due to not only the extensive variety of carbonaceous materials with entirely different properties for the development of a catalyst (powers, fibers, cloths, felts, monoliths, and nanostructured materials) [5–9], but also the possibility that they offer in tailoring textural and surface chemical properties to specific needs [1,2,10]. However, the morphology or structure of the carbonaceous material has also an important role both on the distribution and on the location of the anchoring sites, either intrinsic or produced by a specific method [5], and the interaction degree between the support and the different metallic species involved in the steps of catalyst preparation [1,3,11]. As already evidenced by many authors [1–3,12–17], the latter effect is very important, since the design of the electronic and geometric structure of the specific active sites is an essential factor that determine the catalytic properties.

Transition metals on carbon catalysts are mainly used in hydrogenation, dehydrogenation, or oxidation reactions in fine chemicals area [1,5,18]. One of these reactions is the selective hydrogenation of α,β-unsaturated aldehydes to produce unsaturated alcohols which are used as flavors, fragrances, and intermediaries in the manufacture of drugs with an important industrial interest [19,20]. For this reaction, several transition metals (Ir, Ru, Os, Pd, Ni, Co, and Pt) have been used to prepare catalysts [18,21,22]. Although it is well known that the role of these active metals in the production of adsorbed atomic hydrogen to be added to unsaturated bonds, they are not intrinsically selective to produce unsaturated alcohols, in these cases being thermodynamically favored the C=C hydrogenation over C=O one [18,22]. In general, monometallic catalysts usually produce saturated aldehydes, and it is necessary to modify them either by support effects,

* Corresponding author.
E-mail address: jstassi@fiq.unl.edu.ar (J.P. Stassi).

0021-9517/$ - see front matter © 2013 Elsevier Inc. All rights reserved.
http://dx.doi.org/10.1016/j.jcat.2013.05.029

by changes in the metal particle sizes or by addition of a second metal to improve the selectivity toward the hydrogenations of the carbonyl bonds [18,21–25]. In this sense, several bimetallic formulations on different carbons have been developed, taking mainly into account aspects related to the nature of the metal precursors and the variables concerning the preparative procedures of the catalysts, and tested in selective hydrogenation with different substrates of α,β-unsaturated aldehydes [12,18,26–36]. However, the specific role of the nature of support in the preparation of bimetallic catalysts on carbon has received less attention. There are two main aspects to be considered, which are greatly affected by the characteristics of the support: (i) the oxidation state of the promoter in the final catalyst and (ii) the possibility of alloy formation. In this sense, it has been reported that the use of a relatively inert support as carbon could avoid strong promoter metal–support interactions, thus facilitating the promoter–active metal interactions and leading to an easy reduction in the promoter and formation of alloy phases [1,3,11,35]. However, in spite of these theoretical aspects, most of the studies indicate that, independently of the support and the type of promoter used, the compound containing cations (like Fe, Sn, Ga, Ge, In, Pb, etc.) remain in a major fraction unreduced on the surface as electron-acceptor species and act as adsorption site coordinating the oxygen atom of the unsaturated aldehyde and easing the hydrogenation of carbonyl group by hydrogen atoms chemisorbed on the nearby active metal [22–25,28,29,35,36]. Thus, most of the results seem to be focused mainly in the hypothesis based on the presence of a high proportion of ionic species of the promoter together with the active phase to explain the improvement in the selectivity to unsaturated alcohols.

The aim of this paper is to contribute to a better understanding of the role of the nature of the carbonaceous materials on precursor–support and metal–support interactions and its possible effects on the activity and selectivity in the hydrogenation of α,β-unsaturated aldehydes. H_2PtCl_6, $SnCl_2$, and $FeCl_3$ metallic precursors and two carbonaceous materials (multiple wall carbon nanotubes and carbon Vulcan) have been selected to prepare PtSn and PtFe bimetallic catalysts. Besides, the hydrogenation of citral was chosen as model reaction because this substrate is an interesting α,β-unsaturated aldehyde which has an isolated unsaturated double C=C bond in addition to the double C=C bond conjugated with the carbonyl group. Even though PtFe and PtSn bimetallic catalysts supported on activated carbon were used in selective hydrogenation [18], it must be noted that these bimetallic couples have been less studied on carbon blacks and graphitic materials for the same reaction [12,13,18,37–39]. In this sense, it must be also noted that carbon Vulcan and carbon nanotubes have different electronic and structural properties than activated carbon [5,8,40–43]. Moreover, it must be emphasized that although Vulcan is a granulated carbon black which has a low production cost, high availability, and good textural properties to deposit metals, draw attention that it is widely used as support to prepare fuel cells catalysts [42,43], but practically, there are no studies of selective hydrogenations of α,β-unsaturated aldehydes with this support. According to our knowledge, there are two works about selective hydrogenation of α,β-unsaturated aldehydes with Pt monometallic catalysts supported on carbon Vulcan [44,45]. On the other hand, carbon nanotubes are a kind of nanostructured materials of more recent appearance [7,8] which have exceptional physicochemical properties making them attractive as catalytic support [7,46,47]. This material has been rather used in the area of selective hydrogenation [48–54]. However, except our previous work [55], there are only a few papers that report the citral hydrogenation over metals deposited on carbon nanotubes, which do not use bimetallic catalyst, and they are not focused in obtaining high selectivities to unsaturated alcohols [44,56–60]. Thus, in this paper, we prepare bimetallic catalysts (PtSn and PtFe) on the selected supports and evaluate their catalytic behavior in the citral selective hydrogenation. This work refers to the production of the unsaturated alcohols (geraniol and nerol) with very high selectivities, showing a different point of view with respect to the fundament found in the bibliography about the effect of the metallic promoter on the selectivity to unsaturated alcohols with bimetallic catalysts.

2. Experimental

The two carbonaceous supports selected to prepare the bimetallic catalysts were as follows: (i) commercial multiple wall carbon nanotubes (MWCN from Sunnano, purity >90%, diameter: 10–30 nm, length: 1–10 μm), which were called CN, and (ii) carbon Vulcan XC-72 (from Cabot Corp., purity >99%), which was called CV.

The elementary analysis of the impurities of the carbonaceous materials was carried out by EDX. The original inorganic impurity content of the carbon nanotubes was 6.25 wt% (Fe: 2.779; Al: 2.021; Cl: 0.860; Si: 0.336; S: 0.101 and Ca: 0.051 wt%) while for carbon Vulcan was 0.45 wt% (Fe: 0.005; Al: 0.012; Si: 0.070; S: 0.250; Ca: 0.049; Mg: 0.012; K: 0.005 and Zn: 0.046 wt%). In order to eliminate inorganic impurities, the CN support was purified by successive treatments with aqueous solutions (10 wt%) of HCl, HNO_3, and HF, at room temperature for 48 h without stirring [34,55]. It was used a volume of acid solution/mass of support ratio of 30 mL g^{-1}. After HCl and HNO_3 treatments, the support was filtered and repeatedly washed with deionized water up to a final pH = 4. After the HF treatment, the carbonaceous material was filtered and washed with deionized water up to the same pH of the washing water. Then, the support was dried at 120 °C during 24 h and finally crushed to a powder. The so-purified support was named CN-P. It must be noted that after the treatment with inorganic acids, the impurity content of carbon nanotubes was dramatically reduced. The final impurity content for the CN-P was 0.45 wt% (Fe: 0.2136; Cl: 0.2349; Al: 0.0111; Si: 0.0103; S: 0.0036; Cr: 0.0031; Ca: 0.0029; Ni: 0.0025; and K: 0.0007 wt%).

2.1. Support characterization

2.1.1. Textural characteristics

The specific surface area (S_{BET}) and the pore volume of the different supports were determined by N_2 adsorption at −196 °C in a Quantachrome Corporation NOVA-1000 equipment. Before obtaining adsorption isotherms, the samples were outgassed at 130 °C.

2.1.2. Surface chemistry

The surface chemistry of the different samples was determined by temperature-programmed desorption (TPD) experiments, which were carried out in a differential flow reactor coupled to a thermal conductivity detector. Approximately 300 mg of each sample was stabilized with He at room temperature for 1 h before the TPD experiment. Then, the sample was heated in an electric furnace at 6 °C min^{-1} from 25 to 750 °C. During the TPD experiments, He was passed through the reactor with a flow rate of 9 mL min^{-1}.

2.1.3. Isoelectric point

The isoelectric points of different carbonaceous materials were obtained in aqueous solution of KNO_3. The equilibration was performed under a nitrogen atmosphere to eliminate the influence of atmospheric CO_2 [55]. Thus, the aqueous solution of KNO_3 (0.1 N) was stirred, and purificated N_2 was bubbled through the system at room temperature. The pH of the solution was kept constant (pH = 7) by using nitric acid o potasium hydroxide. Then, the

samples (0.500 g) were suspended into the aqueous solution and allowed to equilibrate, thus obtaining the corresponding value of the isoelectric point.

2.2. Preparation of the catalysts

Monometallic catalysts were prepared by conventional impregnation of the supports (CN-P or CV) using an aqueous solution of H_2PtCl_6 at room temperature for 6 h. The total Pt amount in the impregnating solution was the appropriate to obtain a Pt loading of 5 wt%. In all cases, the conditions to carry out the impregnation of the carbon with the metallic precursor were such as to obtain an homogeneous wetting of these materials and an uniform contact between the solid and the impregnating solution. Thus, a stirring rate of 250 rpm was used for an impregnating volume/support weight ratio of 30 mL g^{-1}. First, the corresponding portion of the solvent was added to the support, and once the carbon was completely wet, the solution of the metallic precursor was introduced. The excess of solution was slowly evaporated after impregnation. Then, the samples were dried at 120 °C overnight, and then, the supports were crushed to a powder.

PtFe bimetallic catalysts over both supports were prepared by coimpregnation of the corresponding precursors using the same conditions above mentioned for monometallic catalysts. Thus, each support was impregnated with a solution containing H_2PtCl_6 and $FeCl_3$. The concentrations of the metallic precursors in the impregnating solution were such as to obtain the desired loadings in the catalysts (Pt: 5 wt% and Fe: 0.35, 1.0, 1.5, 2.5, or 3.5% wt%). Finally, the samples were dried at 120 °C overnight, and then, the catalysts were crushed to a powder.

The bimetallic catalysts of Pt(5 wt%) and Sn (0.5, 1, 2, 3 or 4 wt%) on the corresponding carbonaceous support were prepared by successive impregnation of the monometallic ones. Thus, the precursor of the monometallic catalyst was impregnated for 6 h at room temperature, using a volume of impregnation/mass of support ratio of 30 mL g^{-1} and an hydrochloric solution of $SnCl_2$. In each case, the Sn concentration was such as to obtain 0.5, 1, 2, 3, or 4 wt%. Then, the samples were dried at 120 °C overnight, and then, the catalysts were crushed to a powder.

After conventional impregnation, all catalysts were reduced at 350 °C under hydrogen flow for 3 h. Additionally, some catalysts were submitted a different reductive treatment in order to induce a sinterization of the metallic phase. This reductive treatment consisted of a initial reduction at 350 °C in a H_2 flow for 3 h followed by a thermal treatment under nitrogen flow at 700 °C for 12 h [55]. These catalysts were referred in the text by the denomination of the corresponding catalyst followed by $-N_2$.

All the characteristics of the prepared catalysts according to the preparation method are shown in Table 1.

2.3. Characterization of the catalysts

2.3.1. Test reactions of the metallic phase

Two test reactions were carried out on catalytic samples: cyclohexane dehydrogenation (CHD) and cyclopentane hydrogenolysis (CPH). Both reactions were performed in a differential continuous flow reactor at atmospheric pressure by using a H_2-reaction substrate gaseous mixture and a volumetric flow of 600 mL min^{-1}. For CHD, the reaction temperature was 250 °C and the H_2/CH molar ratio equal to 26; for CPH, the temperature was of 350 °C and the H_2/CP molar ratio equal to 29. In both reactions, the catalysts were previously reduced "in situ" in flowing H_2 at 350 °C for 3 h. The catalyst weight used in these test reactions was the appropriate one to obtain a conversion lower than 5%, since under these conditions, the behavior of the reactor follows a differential flow reactor model allowing the correct measurement of the initial rate and activation energy. The reaction products and the remaining reactants were analyzed by a gas chromatographic system. The activation energy values for CHD (Ea_{CH}) were calculated by linear regression using the reaction rates measured at three temperatures (250, 240, and 230 °C) and the Arrhenius plot ($\ln r_{oCH}$ versus $1/T$ (K^{-1})).

2.3.2. Hydrogen chemisorption

The H_2 chemisorption measurements were carried out in a volumetric equipment at room temperature. The sample weight used in the experiments was 200 mg. In these experiments, the catalysts were previously reduced in H_2 at 350 °C for 3 h, then outgassed under high vacuum (10^{-5} Torr) at the same temperature for 1 h, and finally cooled down to room temperature. The H_2 adsorption isotherms were performed at room temperature between 25 and 100 Torr. The isotherms were linear in the range of used pressures and the H_2 chemisorption capacity was calculated by extrapolation of the isotherms to zero pressure [61].

2.3.3. Temperature-programmed reduction

Temperature-programmed reduction (TPR) experiments were performed by using a reductive mixture of H_2 (5%v/v)–N_2 and a flow rate of 9 mL min^{-1} in a flow reactor. Samples (approximately 200 mg) were heated at 6 °C min^{-1} from 25 to 800 °C. Before TPR experiments, the impregnated samples were stabilized with N_2 at room temperature for 1 h.

2.3.4. X-ray photoelectron spectrometry (XPS)

XPS determinations were carried out in a Multitechnic Specs photoemission electron spectrometer, equipped with an X-ray source Mg/Al and a hemispherical analyzer PHOIBOS 150 in the fixed analyzer transmission mode (FAT), operating with an energy power of 100 eV. The spectra were obtained with a pass energy of 30 eV and a Mg anode operated at 100 W. The pressure of the analysis chamber was lower than 5×10^{-8} mbar. Samples prepared by conventional impregnation were previously reduced under H_2 at 350 °C for 3 h in a flow reactor, and then, they were introduced in the equipment and reduced "in situ" with H_2 at 350 °C for 1 h. Peak areas and BE values were estimated by fitting the curves with combination of Lorentzian–Gaussian curves of variable proportion using the CasaXPS Peak-fit software version 1.2. In order to determine the peak position accurately, the BE values of the energy levels of the corresponding atoms species were referenced to the C 1s binding energy of 284.6 eV. Besides, to fit correctly the Pt 4f spectra of the different catalysts, the corresponding deconvolutions were performed assuming an intensity ratio of Pt $4f_{7/2}$ to Pt $4f_{5/2}$ of 1:0.75, and a separation between the Pt 4f doublet signals of 3.36 eV [62].

2.4. Citral hydrogenation

The different catalysts were tested in the citral hydrogenation at 70 °C and atmospheric pressure in a discontinuous glass reactor equipped with a device for withdrawing samples from the slurry during the course of the reaction without stopping the stirring using a septum device. In each experiment, 0.3 mL of citral (Aldrich, 61% cis and 36% trans) was hydrogenated by using 0.300 g of catalyst and 30 mL of solvent (2-propanol). The reaction mixture was stirred at 1400 rpm (in order to minimize the limitations of the mass transfer steps) since from previous experiments, diffusional limitations were found to be absent under these conditions. After the reaction system was purged, the reduction in the catalysts was carried "in situ" under flowing H_2 at 350 °C for 3 h, prior to the reaction, and then, they were cooled down to the reaction temperature. The typical procedure to start the reaction was as follows: introduction of H_2 (at low pressure), introduction of the

Table 1
Characteristics of the studied catalysts.

Catalysts designation	Preparation method	Sn(wt%) or Fe(wt%)	Sn/Pt or Fe/Pt atomic ratio
Pt(5wt%)/CN-P Pt(5wt%)/CV	(1) Conventional impregnation (2) Reductive treatment in H_2 flow at 350 °C	–	–
Pt(5wt%)Fe(Ywt%)/CN-P Pt(5wt%)Fe(Ywt%)/CV	(1) Conventional impregnation (co-impregnation of metallic precursors) (2) Reductive treatment in H_2 flow at 350 °C	(*Y*) = 0.35, 0.99, 1.5, 1.8, 2.5, or 3.5.	0.25, 0.66, 1.05, 1.26, 1.75 or 2.48, according to the corresponding value of (*Y*)
[Pt(5wt%)Fe(2.5wt%)/CN-P]-N_2 [Pt(5wt%)Fe(2.5wt%)/CV]-N_2	(1) Conventional impregnation (2) Reductive treatment in H_2 flow at 350 °C (3)Thermal treatment with N_2 at 700 °C	2.5	1.75
Pt(5wt%)Sn(Xwt%)/CN-P Pt(5wt%)Sn(Xwt%)/CV	(1) Conventional impregnation (successive impregnation of metallic precursors) (2) Reductive treatment in H_2 flow at 350 °C	(X)=0.5, 1, 2, 3, or 4.	0.16, 0.33, 0.67, 0.99, or 1.31, according to the corresponding value of (*X*)
[Pt(5wt%)Sn(1wt%)/CN-P]-N_2 [Pt(5wt%)Sn(3wt%)/CV]-N_2	(1) Conventional impregnation (2) Reductive treatment in H_2 flow at 350 °C (3) Thermal treatment with N_2 at 700 °C	1 or 3	0.33 or 0.99

solvent, heating of the mixture until desired reaction temperature, introduction of a citral adequated amount, increasing of H_2 pressure of until atmospheric pressure, and finally, the zero time was taken when the agitation began. The reaction products were analyzed in a GC system coupled to a capilar column (Supelcowax 10 M) and using a FID detector. All products were identificated by using gas chromatography standards except for 3,7-dimethyloctanal and other secondary products derived of side reactions such as cyclization, decarbonylation, and isomerization. These products were identified by gas chromatography–mass spectrometry (GC–MS) technique. The calculation of the activity and selectivity was made by using the internal normalization methods. The catalytic activity was defined as the sum of percentages of citral converted into different products. The selectivity to a given product (*i*) was calculated as the ratio between the amount of product *i* and the total amounts of products.

3. Results and discussion

3.1. Characteristics of the supports

Table 2 shows results of the textural and acid-basic characteristics of the two carbons selected to prepare catalysts (CN-P and CV) and also of the nanotubes without purification treatment (CN): BET surface area (S_{BET}), pore volume (V_{pore}), and isoelectric points (IP) values. As it is observed, S_{BET} and V_{pore} values for CN support do not decrease in an important way after purification treatment of the nanotubes, the diminution of these values being of approximately 15% both of S_{BET} and V_{pore}. However, it should be noted that S_{BET} and V_{pore} values for CN-P support are lower than the corresponding to CV support (about 26% for S_{BET} and 22% for V_{pore}), thus indicating a difference in the textural properties of both support used to prepare the catalysts.

Table 2
Surface area (S_{BET}), pore volume (V_{pore}) and isoelectric points (IP) of carbon Vulcan and carbon nanotubes with and without purification.

Support	S_{BET} ($m^2\ g^{-1}$)	V_{pore} ($cm^3\ g^{-1}$)	IP
CN	211	0.46	4.6
CN-P	179	0.39	4.7
CV	240	0.36	7.4

To interpret the change in the S_{BET} and V_{pore} values of CN support after its purification, it must be considered that, in addition to the elimination of inorganic impurities, the treatment with inorganic acids could oxidize and functionalize the surface of the carbon with the development of surface oxygenated groups [48]. In this sense, the change in the textural properties in CN support was attributed to a balance between opposite effects produced by the oxidative treatment on their intrinsic structure, such as partial destruction of micropores and walls with diminution of the surface area, and opening of closed tips blocked by Fe particles with elimination of these particles, this last effect producing an increase in the surface area [55].

Table 2 also shows the values of isoelectric points (IP) of the different supports. From these results, it is observed that the purification treatment done on CN sample does not practically change the isoelectric point value. This result would be indicating a slight change in the distribution of the different surface oxygenated groups over CN-samples [55]. On the other hand, the CV support shows an isoelectric point value practically neutral (IP = 7.4). This result would be evidencing more basic carbon characteristics than CN and CN-P supports, which show an IP of about 4.6–4.7. These results were also evidenced from TPD experiments, which were used to characterize the surface functional groups of different supports. It is known that the oxidation treatments of carbon lead to the formation of different surface acid groups [63]. According to the literature, these surface groups decompose upon heating desorbing CO_2 at low temperatures from stronger acid groups (carboxylic and anhydride groups) and CO at high temperatures from the weaker acid sites (lactone, phenol, and carbonyl groups) [63,64]. Fig. 1 shows the amounts of desorbed CO and CO_2 as a function of temperature for CN, CN-P, and CV samples. It can be observed that the original carbon nanotubes only show a low amount of weak acid groups, while the CV sample does not desorb functional groups. For the CN-P support, it can be observed that the treatment produces the formation of few strong acid groups but an important formation of weak acid ones.

Thus, from the results of support characterization, it can be concluded that the supports show quite similar textural properties but different acid-basic properties, which could be related to the different structures of these materials. Both supports exhibit a mesoporous and macroporous structure with a small amount of micropores [40,41,43,50] and a reasonably high surface area to disperse high loadings of metal phase [7,43]. On the one hand, carbon nanotubes show a high external surface area which it is provided by the high

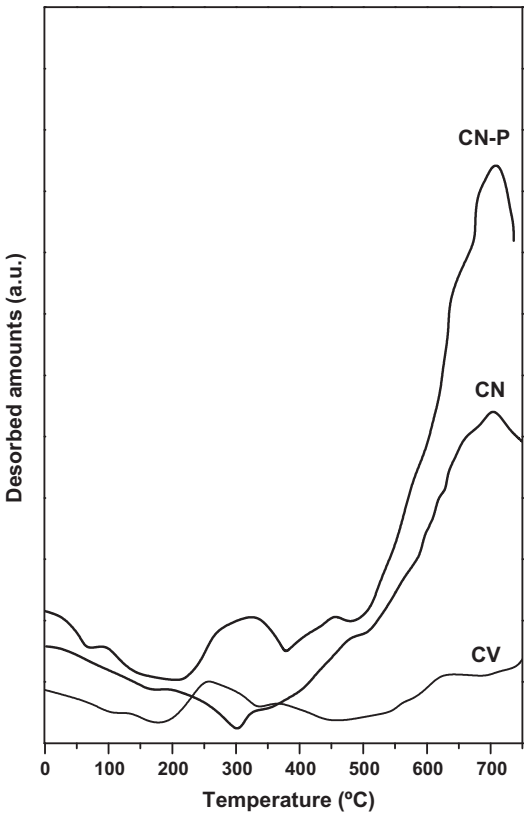

Fig. 1. TPD profiles of the supports: CV, CN, and CN-P.

length-to-diameter ratio. Besides, this structure could be easily functionalized in unsaturated sites, i.e., at defects, and these sites could contribute to the acidity of the support. On the other hand, in carbon Vulcan, the secondary structure of spheric aggregates is controlled by certain groups of heteroatoms placed in the perimeter of the each basal plane. These functional groups at the edges of the basal plane structures, including oxygenated groups, must not be very acid since they allow the stabilization of the aggregates. In effect, carbon Vulcan does not show desorption of functional groups from TPD experiments, thus indicating the presence of strong basic groups which could be desorbed at higher temperatures than those reached in these experiences.

3.2. Characteristics of the metallic phases

3.2.1. TPR profiles

Fig. 2 shows the TPR profiles for the PtSn and PtFe bimetallic catalysts series supported on CN-P and CV carbons. Besides, for the sake of comparison, TPR profiles of CN-P and CV supports and Fe(2.5wt%)/CV, Fe(2.5wt%)/CN-P, Sn(3wt%)/CV, and Sn(3wt%)/CN-P samples are also included in the corresponding catalytic series.

It can be observed in Fig. 2A and C that the CN-P profile displays only one H_2 consumption zone at temperatures higher than 400 °C, which is coincident with the zone of CO-desorption in TPD experiments (see Fig. 1). Thus, this broad peak of H_2 consumption would be related to the decomposition of functional groups of the support producing CO-desorption and the simultaneous creation of unsaturated reactive surface sites able to interact with hydrogen at high temperatures [32,55,64,65]. On the other hand, the CV profile showed in Fig. 2B and D also displays only one H_2 consumption broad zone at high temperatures (above 500 °C), although it shows a minor intensity compared with that corresponding in the CN-P profile. In spite of this, it must be noted that this support does not show any desorption of acid functional groups from TPD experiments at the same temperature range. These results reveal that other sites (basic or weakly acid), which do not desorb as CO from TPD experiments, would be present on this support, and they could interact with hydrogen at high temperatures [10,63,66].

Fig. 2A and B shows the TPR profiles of PtFe catalyst series prepared on CN-P and CV supports, respectively. TPR profiles of the CN-P-based PtFe catalysts are quite similar to those CV based: all the profiles show an important peak of reduction at about 180–200 °C, additional peaks or H_2 consumption zones at temperatures between 250 and 550 °C, and a desorption zone at temperatures higher than 550 °C. It can be also observed that Fe(2.5wt%)/CN-P and Fe(2.5wt%)/CV samples display two similar H_2 consumption zones at high temperatures: one broad peak between 350–700 °C and a shoulder at approximately 625–675 °C. The reduction temperature of the second peak in both Fe samples is coincident with the maximum of the broad peak above described for TPR profiles of the corresponding supports. Besides, it must be noted that the first broad peak has a maximum at about 480 °C in the Fe(2.5wt%)/CV profile and about 510 °C in the corresponding profile of the Fe(2.5wt%)/CN-P sample, which could be caused by the existence of different ionic species of Fe created during the impregnation step, or also due to a different interaction of the Fe with each support. These H_2 consumption zones were assigned to the reduction of ionic Fe [26,47,55,67]. On the other hand, TPR profiles of the Pt monometallic catalysts supported on CN-P and CV show a reduction peak with a maximum at about 180–200 °C that would correspond to the reduction of the deposited metal complex to zerovalent state [26,27,34,67]. Additionally, these profiles show peaks or H_2 consumption zones at temperatures higher than 250 °C which can be explained due to the existence of other effects produced by the thermal treatment with hydrogen during the TPR experiment [32,64,65]. In this sense, it must be noted that the H_2 consumption zones between 375 and 550 °C for both monometallic catalysts were also observed in the TPR profiles of the corresponding supports, but these zones appear at higher temperatures. This fact would be indicating that the presence of Pt would produce a catalytic effect on the decomposition of the functional groups present in each support. Besides, the small shoulder between 275 and 375 °C in Pt/CN-P catalyst would also be indicating a catalytic effect since the TPR profile of CN-P support does not show a H_2 consumption beneath 400 °C even when it was observed a small desorption of strong acid groups from TPD results. The profiles of both series of PtFe bimetallic catalysts supported on CN-P and CV supports show an important reduction peak in the zone of Pt reduction in the corresponding monometallic catalyst (about 180–210 °C). However, it should be differentiated between both series that there only is a shift (although not too much significative) in the reduction temperature of the Pt precursor for PtFe series supported on CV. Besides, it is also observed for both series that the higher the Fe loading added to the monometallic catalyst, the higher the H_2 consumption in this zone. This effect would be related both to the Pt reduction and a simultaneous catalytic effect of the Pt on the Fe reduction to a lower oxidation state than of the precursor, or up the zerovalent state. Besides, it must be noted that all the bimetallic samples display one small and broad additional peak at high temperatures (above 400–500 °C) and an intermediate reduction zone between this peak and the Pt reduction one. The H_2 consumption of these zones increases when the Fe loading increases in the samples. The intermediate reduction zone could be due not only to a reduction catalytic effect of Pt with some fraction of Fe, which would present in the vicinity of the Pt, but also the reduction of sites produced by decomposition of functional groups of the supports. The reduction zone at higher temperatures is coincident with the Fe reduction

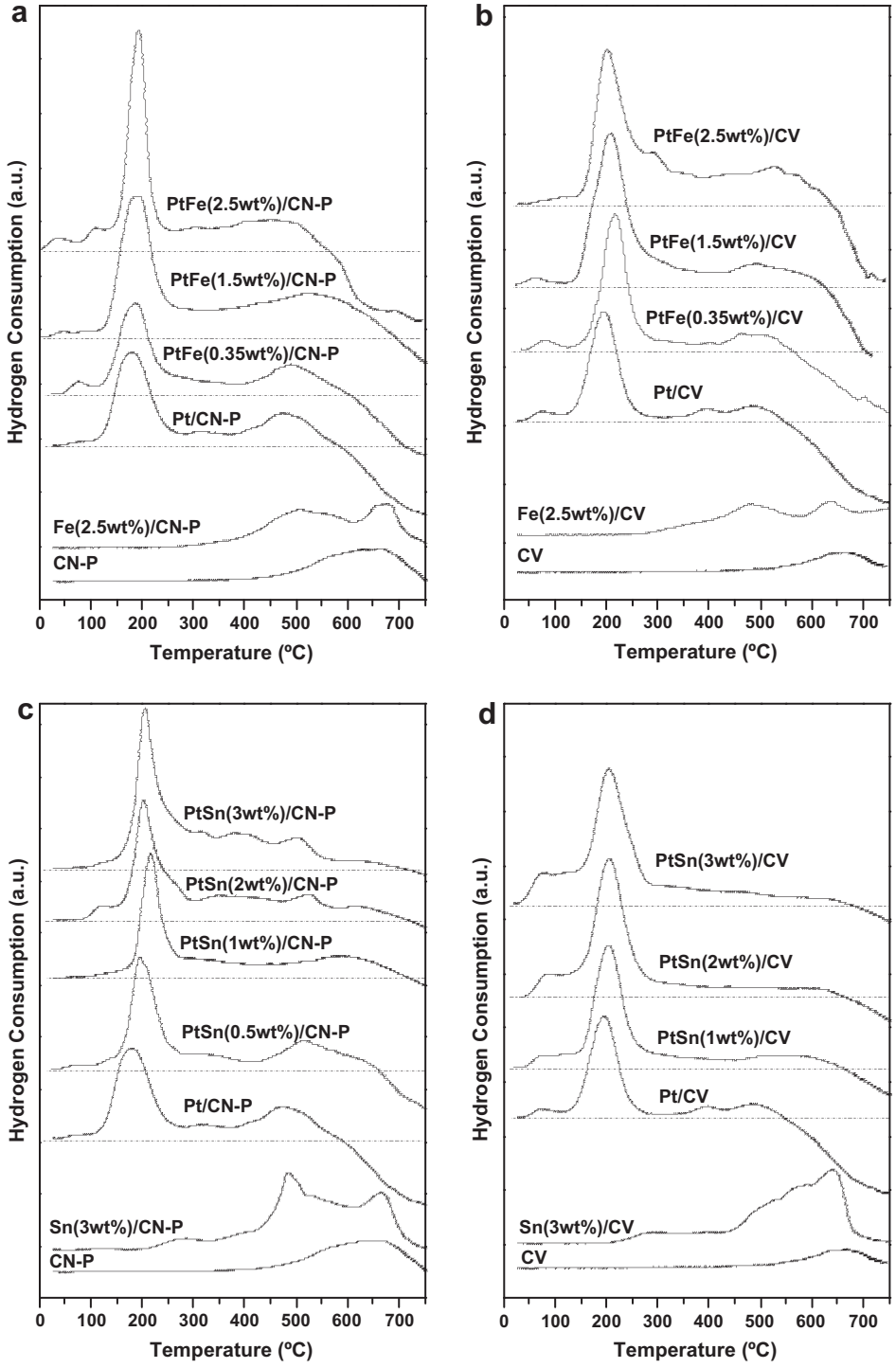

Fig. 2. TPR profiles for the different bimetallic catalytic series. (A) PtFe/CN-P, (B) PtFe/CV, (C) PtSn/CN-P, and (D) PtSn/CV.

zone, thus indicating that the higher the content of Fe, the higher the fraction of Fe that could remain as ionic species stabilized on the support at the temperature of catalyst reduction (350 °C) before reaction.

Fig. 2C and D shows the TPR profiles of PtSn catalyst series prepared on CN-P and CV supports, respectively. TPR profiles of CN-P-based and CV-based PtSn catalysts show some differences respect to PtFe bimetallic ones. In these cases, it can be observed that the Sn reduction profiles of Sn(3wt%)/CN-P and Sn(3wt%)/CV samples begin at low temperature (about 250 °C) with a small intensity and finish at high temperature with a notorious increase in the intensity. These reduction zones at higher temperatures overlap the H_2 consumption zones at high temperatures observed in the corresponding supports. On the other hand, when the profiles of the PtSn bimetallic catalysts are analyzed in comparison with the profiles of the corresponding Pt or Sn monometallic samples, interesting results can be observed. First, in both catalytic series, the Pt reduction peak in bimetallic samples is shifted to higher temperatures with respect to those corresponding to the monometallic catalyst. Besides, it must be noted that this shift is higher in the series of

catalysts supported on CN-P (from 180 to 215 °C) than in the series of catalysts supported on CV (from 190 to 210 °C). Second, in both series, the H_2 consumption amount increases as the Sn loading increases. Third, in all bimetallic samples, it is observed a small and broad H_2 consumption zone without significant maximum in samples supported on CV, and with a higher intensity in the series of bimetallic samples supported on CN-P, from about 300 °C to about 650–700 °C. Finally, contrary to what was observed for the monometallic samples and PtFe bimetallic series, the TPR profiles of PtSn series do not show a significative desorption zone at high temperatures, these being practically negligible a high Sn loading.

Thus, all these results from PtSn series would be evidencing that an important co-reduction of the both metals (Pt and Sn) occurs, and also that reduced Sn could be present in the metallic phase opening the possibility to the formation of alloy phases between metallic platinum and metallic tin. This co-reduction effect seems to be more marked in bimetallic samples on CV, since these catalysts show a H_2 consumption zone practically negligible at temperatures where Sn is reduced. Besides, it must be noted that different Sn species (ionic and/or reduced) could be present both in the vicinity of the Pt and on the support as free Sn species. However, it must be emphasized that, on CV support, the amount of free Sn species seems to be significantly lower than on the CN-P one. As it is already known, Pt particles can act as adsorption sites for hydrogen which once dissociated, is spilt over the carbon surface being retained over it or occupying the reactive sites formed upon the decomposition of surface oxygenated groups [27,55,64,65,68,69], but it also can be used to reduce Sn ionic species [70]. In this sense, it must be noted that the partial reduction of the support could have an important role on the metal–support interaction, thus modifying the interaction of Sn with carbon and favoring the Sn reduction and/or the mobility or migration of Sn species from the support toward the vicinity of the Pt particles [32,68]. So, in these PtSn bimetallic series, it could be postulated that the hydrogen dissociated by reduced Pt during the TPR experiments is mainly used to reduce the support and Sn and also that it is less retained over the carbon surface. In fact, the hydrogen desorbed from the bimetallic catalysts is lower than the monometallic samples, as it was above mentioned.

3.2.2. Test reactions of the metallic phase and H_2 chemisorption

In order to find more evidences about the Pt–promoter interaction in catalysts prepared on CN-P and CV supports, test reactions (cyclohexane dehydrogenation –CHD– and cyclopentane hydrogenolysis –CHD–) of the metallic phase and H_2 chemisorption measurements were carried out. Tables 3 and 4 show the results of these characterization techniques for both bimetallic catalyst series: initial reaction rate (R^o_{CH}) and activation energy (Ea_{CH}) values for CHD, values of initial reaction rate (R^o_{CP}) for CPH and H_2 chemisorption capacities (H). It should be noted that the CHD is a structure-insensitive reaction [71], which involves only one metallic Pt exposed site, while the CPH is a structure-sensitive reaction [72], which is carried out on ensembles of a certain number of active atoms. For CHD, two parameters are important: the reaction rate, since it can be taken as an indirect measurement of exposed surface Pt atoms, and the activation energy, since its value can be modified if the nature of the metallic site is changed by some effect, such as, the presence of a second metal or the different properties of the support (electronic modification in the metal–metal or metal–support interaction). For CPH, a change in the reaction rate can be also observed if a modification of the metallic phase is produced by some geometric or electronic effects. Indeed, the reaction rate is decreased when the addition of a second metal to Pt reduces the concentration of the ensembles necessary for this reaction.

3.2.2.1. PtFe catalyst series. Table 3 shows the behavior of both PtFe catalytic series (supported on carbon nanotubes and carbon Vulcan) in the test reactions and their hydrogen chemisorption capacities. It can be observed from these results that the Fe addition to Pt in catalysts supported on carbon nanotubes modifies in an important degree both the in CHD and CPH reaction rates and the H_2 chemisorption values. In this sense, the R^o_{CH} and R^o_{CP} values for the catalyst with the highest Fe content decrease about 72% and 45%, respectively, with respect to the monometallic one, and a higher diminution of chemisorbed hydrogen was also observed (about 93%) for the same catalyst with respect to the monometallic one. Besides, it can also be noted that the reaction rates proportionally decrease with the increase in the Fe amount added to Pt, while there is an abrupt diminution of the values of H_2 chemisorption in these catalysts. With respect to the activation energy values for CH dehydrogenation reaction, they slightly increase as the Fe amount added to Pt increases. Taking into account the insensitive character of the CH dehydrogenation reaction, the low modification of the activation energy and the important decrease in the initial activity would indicate a poor electronic modification of Pt by Fe. Hence, the decrease of R^o_{CH}, R^o_{CH}, and H, would evidence an important geometric modification of the metallic phase by dilution or blocking of the surface Pt atoms in this series. Table 3 also shows the results for PtFe bimetallic catalysts supported on carbon Vulcan. It can be observed that R^o_{CH} and R^o_{CP} values are not modified in an important way in all the bimetallic catalyst series. These values only decrease about 15–30% and remain practically unmodified by the Fe loading. The activation energies of CH dehydrogenation for bimetallic catalysts supported on carbon

Table 3
Initial reaction rates of CHD (R^0_{CH}) and CPH (R^0_{CP}), activation energy in CDH (Ea_{CH}) and H_2 chemisorption capacity (H) for PtFe catalyst series.

Catalyst	R^0_{CH} (mol/h g Pt)	Ea_{CH} (kcal/mol)	R^0_{CP} (mol/h g Pt)	H (mol/g cat.)
Pt(5wt%)/CN-P	1.78	41	8.87	38.05 [a] (D = 29.8)
Pt(5wt%)Fe(0.35wt%)/CN-P	1.68	43	7.69	26.42
Pt(5wt%)Fe(0.95wt%)/CN-P	1.41	44	6.55	n.d.
Pt(5wt%)Fe(1.5wt%)/CN-P	1.35	46	5.40	4.08
Pt(5wt%)Fe(2.5wt%)/CN-P	0.85	43	4.92	2.64
Pt(5wt%)Fe(3.55wt%)/CN-P	0.49	48	n.d.	<0.1
[Pt(5wt%)Fe(2.5wt%)/CN-P]-N_2	0.28	48	0.72	<0.1
Pt(5wt%)/CV	0.71	40	6.30	34.75[a] (D = 27.2)
Pt(5wt%)Fe(0.35wt%)/CV	0.51	65	4.24	21.48
Pt(5wt%)Fe(1.5wt%)/CV	0.62	60	4.15	11.40
Pt(5wt%)Fe(2.5wt%)/CV	0.61	59	4.54	3.60
Pt(5wt%)Fe(3.55wt%)/CV	0.62	60	n.d.	<0.1
[Pt(5wt%)Fe(2.5wt%)/CV]-N_2	0.27	52	0.32	1.72

n.d.: Not determined.
[a] D = Pt dispersion.

Table 4
Initial reaction rates of CHD (R^0_{CH}) and CPH (R^0_{CP}), activation energy in CDH (Ea_{CH}) and H_2 chemisorption capacity (H) for PtSn catalyst series.

Catalyst	R^0_{CH} (mol/h g Pt)	Ea_{CH} (kcal/mol)	R^0_{CP} (mol/h g Pt)	H (mol/g cat.)
Pt(5wt%)/CN-P	1.78	41	8.87	38.05[a] (D = 29.8)
Pt(5wt%)Sn(0.5wt%)/CN-P	0.75	47	1.63	5.28
Pt(5wt%)Sn(1wt%)/CN-P	0.74	49	0.77	2.70
Pt(5wt%)Sn(2wt%)/CN-P	n.d.	n.d.	0.38	0.97
Pt(5wt%)Sn(3wt%)/CN-P	0.13	58	0.21	0.37
[Pt(5wt%)Sn(1wt%)/CN-P]-N_2	<0.1	n.d.	0.28	<0.1
Pt(5wt%)/CV	0.71	40	6.30	34.75[a] (D = 27.2)
Pt(5wt%)Sn(1wt%)/CV	0.54	48	1.55	21.26
Pt(5wt%)Sn(2wt%)/CV	0.36	53	0.21	10.99
Pt(5wt%)Sn(3wt%)/CV	0.17	55	0.29	3.75
Pt(5wt%)Sn(4wt%)/CV	<0.1	n.d.	0.26	0.39
[Pt(5wt%)Sn(3wt%)/CV]-N_2	<0.1.	n.d.	0.26	0.54

n.d.: Not determined.
[*] D = Pt dispersion.

Vulcan are significatively higher than the corresponding to the monometallic one, and these values also remain practically unmodified by the Fe loading, this behavior being different from the one observed for PtFe catalysts supported on CN-P. This series also shows an important decrease in the H_2 chemisorption values, the chemisorption being practically negligible for a Fe loading of about 3.5%. Since any significative modification of the Ea_{CH} value would be indicating a change in the electronic structure of the catalytic sites, the addition of Fe to Pt over carbon Vulcan would reveal in this case that an important electronic interaction exists between both metals with probable alloy formation. In this sense, it must be noted that in general, the reduced or alloyed promoter species produce a geometric effect in the metallic phase due to these species are not active in the dehydrogenation and hydrogenolysis reactions, and in consequence, it is observed an important decrease in the reaction rates when the activation energy significantly changes, as it was described in the literature [30–33]. However, our results would indicate that, in addition to the probable presence of inactive ionic Fe species nearby to Pt in the metallic phase, the new sites created by electronic interaction between Fe and Pt would be active in the test reactions studied, since the corresponding reaction rates slightly decrease. These results were also confirmed by CHD rate values in ionic or reduced Fe samples supported on the studied carbons, which were negligible. Besides, regarding the H_2 chemisorption capacities corresponding to this catalytic series, the results show that there is a higher decrease in the values than in the CHD activity. Taking into account the above-mentioned comments and the geometric effect produced by Fe species, these results can be explained considering that there would exist different structural requirements for the H_2 chemisorption with respect to the cyclohexane dehydrogenation [73,74].

3.2.2.2. PtSn catalyst series. Table 4 shows the results of the test reactions of the metallic phase and the hydrogen chemisorption capacities of the PtSn catalytic series supported on carbon nanotubes and carbon Vulcan. From these results, it can be observed a quite similar behavior for both series in these experiments with the addition of Sn to the corresponding monometallic catalysts. Thus, the Sn addition to the parent Pt catalyst produces a sharp decrease in both reaction rates (R^o_{CH} and R^o_{CP}) when the Sn content increases (being approximately 10 times for the highest Sn loading). Furthermore, the activation energies of CH dehydrogenation for bimetallic catalysts significantly increase as the added Sn loading increases. It can observed that the H_2 chemisorption capacities also decrease with the addition of Sn to the corresponding monometallic catalyst, this decrease taking place in both series and reaching more than one order of magnitude for the highest Sn loading. Taking into account both the great drop of the specific activity in CHD and the important increase in the activation energy of PtSn catalysts with respect to the corresponding Pt samples, these results would indicate a strong electronic interaction between both metals. Besides, the sharp decrease in the catalytic activity for CPH reaction indicates that there is a strong diminution of the concentration of Pt atom ensembles required for this reaction. So, according to these results, dilution and/or blocking effects of Sn on Pt particles would be associated with the alloy formation in both PtSn catalytic series, as it can be also inferred from H_2 chemisorption results. These results are also in agreement with TPR experiments which show that practically all the Sn is co-reduced together with Pt in these bimetallic series. It must be pointed out that contrary to the results observed for PtFe on carbon Vulcan, the possible presence of alloy phases in PtSn catalysts does not necessarily imply activity of these species in test reactions. These results are in agreement with those reported in the literature [75,76].

Tables 3 and 4 also show the results found for [Pt(5wt%)Fe(2.5wt%)/CN-P]-N_2, [Pt(5wt%)Fe(2.5wt%)/CV]-N_2, [Pt(5wt%)Sn(1wt%)/CN-P]-N_2, [Pt(5wt%)Sn(3wt%)/CV]-N_2 catalysts which were submitted to a thermal treatment under N_2 flow at 700 °C after the conventional reduction in H_2 flow at 350 °C. It is worth noticing that the object of the thermal treatment with N_2 was to modify the concentration of remaining oxygenated groups after the reduction step and simultaneously induce sintering, as it was suggested by us in our previous study with Pt catalysts supported on carbon nanotubes with different surface chemical composition [55]. In these cases, the modification of particle sizes toward larger ones during the treatment with N_2 would produce a decrease in the final fraction of exposed Pt atoms. So, taking into account that the CHD reaction allows an indirect measurement of exposed surface Pt atoms and that the lower the fraction of exposed Pt atoms, the lower the concentration of metallic ensembles necessary for the CPH reaction, it must be expected lower CHD and CPH reaction rates in those catalysts thermally treated with N_2 than in the corresponding parent catalysts without treatment. In effect, [Pt(5wt%)Fe(2.5wt%)/CN-P]-N_2 and [Pt(5wt%)Fe(2.5wt%)/CV]-N_2 catalysts show a lower CHD and CPH reaction rates with respect to the values obtained for the corresponding catalysts without any treatment. Besides, in this sense it was observed, for example, a slight change in the particle average diameter (TEM measurements) from 2.2 to 2.7 nm when Pt(5wt%)Fe(1.5wt%)/CN-P catalyst was treated with N_2 at high temperature [55]. In the same way, [Pt(5wt%)Sn(1wt%)/CN-P]-N_2 and [Pt(5wt%)Sn(3wt%)/CV]-N_2 catalysts also showed an important diminution of the rates after nitrogen treatment, their activities being negligible in CHD reaction. In agreement with these results, the hydrogen chemisorption capacities also decrease both for PtFe and PtSn catalysts on CN-P and CV supports when they are treated with nitrogen.

3.2.3. XPS characterization

XPS spectra corresponding to Pt 4f, Fe 2p, Sn 3d, C 1s, and O 1s core levels of the different mono and bimetallic catalysts supported on CN-P and CV were determined. The binding energies of the Pt $4f_{7/2}$ and Fe $2p_{3/2}$ levels, the percentages of reduced and oxidized species, and the Pt/C and Fe_T/Pt surface molar ratios (Fe_T: total moles of Fe) for the two bimetallic PtFe catalytic series supported on CN-P and CV are reported in Table 5. For bimetallic PtSn catalytic series, the BE values Pt $4f_{7/2}$ and Sn $3d_{5/2}$ levels, percentages of reduced and oxidized species, and surface Pt/C and Sn_T/Pt molar ratios (Sn_T: total moles of Sn) are shown in Table 6.

Fig. 3 shows Pt 4f and Fe 2p XPS spectra of PtFe bimetallic catalysts, and Fig. 4 shows Pt 4f and Sn 3d XPS spectra of other selected PtSn bimetallic catalysts. It can be observed from these figures that there is an asymmetry in the Pt 4f level of these samples at about 76–80 eV. This asymmetry was found in all the reduced catalysts and would be indicating that a certain amount of ionic species of Pt(II) or Pt(IV) would be masked by the major signal from metallic Pt at about 71–72 eV. This fact is not surprising since in a previous study we reported that Pt could form stable species with both the surface oxygenated groups and the other sites of the support, or including with chlorine species, which could remain unreduced at the temperature used for obtaining the final catalyst [55]. These results agree with those in the literature, where many authors have reported the presence of Pt oxide species in a Pt(0):P(ox) ratio of about 75:25 in catalysts prepared over carbon nanotubes and carbon Vulcan [77,78]. Thus, from the deconvolution of Pt 4f XPS spectra in all the catalysts, three doublets were obtained: (i) one at low binding energy, at about 71.6–72.0 eV for Pt $4f_{7/2}$ and the corresponding values for Pt $4f_{5/2}$ shifted at 3.36 eV at higher BE, which can be assigned to zerovalent Pt; (ii) other at about 73.1–73.5 eV for Pt $4f_{7/2}$ and the corresponding values for Pt $4f_{5/2}$ shifted at 3.36 eV at higher BE, assigned to Pt(II); and (iii) a third one at higher binding energy, at about 74.6–76.7 eV for Pt $4f_{7/2}$ and the corresponding values for Pt $4f_{5/2}$ shifted at 3.36 eV at higher BE, assigned to Pt(IV) species. These values are listed in Tables 5 and 6.

From results of Table 5, it can be observed that the percentages of the reduced Pt for the different PtFe bimetallic catalysts of both series supported on CN-P and CV are slightly higher with respect to the corresponding monometallic one, although these values are not practically modified by the Fe loading. Fig. 3 shows the different contributions of the ionic and zerovalent Fe species for both PtFe series. The percentages of these species are also listed in Table 5. From these results, it can be observed that Fe in these series shows different oxidation states according to the type of support. For PtFe bimetallic catalysts supported on carbon nanotubes, Fe is only present as ionic species, except for the catalyst treated with N_2. For PtFe bimetallic catalysts supported on carbon Vulcan, an important fraction of Fe is present as zerovalent state. Besides, it must be noted that the zerovalent Fe binding energy values are in a range of 707.2–707.8 eV. These values are slightly higher than 2p 3/2 binding energy of metallic iron, which was reported at 706.8 eV [79]. This shift toward higher values could be attributed to the formation of PtFe alloy, as it was reported in the literature [53,80].

Regarding Pt/C surface molar ratio, its value can be taken as an estimation of the amount of surface Pt atoms. As it can be observed from Pt/C values in both series, this ratio slightly decreases as the Fe content increases, except for those catalysts treated with N_2, which show a more significative diminution of the values as a possible consequence of the sintering of the metallic particles produced by the thermal treatment. Moreover, when the Fe/Pt surface molar ratio is analyzed in these series, it can be concluded that there is not an important surface enrichment of Fe even with the highest Fe loading (which involved a bulk Fe/Pt molar ratio $\gg 1$). So, the results from Pt/C and Fe/Pt ratios in PtFe catalysts indicate that it would be necessary a Fe high loading to obtain a significative geometric modification (by dilution or blocking) of the Pt metallic phase. Finally, it must be noted that the existence of a fraction of Fe^o in catalysts treated with N_2 (which it is not present in the parent catalysts without treatment) could be caused by a change in the surface chemical composition of the carbon nanotubes during the treatment that could produce a better Pt–Fe interaction.

Table 5
XPS results of the PtFe catalysts series supported on CN-P and CV.

Catalyst	Atomic ratio		Pt $4f_{7/2}$ level			Fe $2p_{3/2}$ level		
	Pt/C	Fe/Pt	BE (eV)	Species	%	BE (eV)	Species	%
Pt(5wt%)/CN-P	0.60	–	71.67	Pt^o	63.6	–	–	–
			73.06	Pt^{2+}	23.6			
			75.95	Pt^{4+}	12.8			
Pt(5wt%)Fe(0.35wt%)/CN-P	0.53	0.89	71.73	Pt^o	69.2	711.12	Fe^{3+}	100
			73.12	Pt^{2+}	19.0			
			75.09	Pt^{4+}	11.8			
Pt(5wt%)Fe(2.5wt%)/CN-P	0.57	0.76	71.83	Pt^o	68.2	710.54.	Fe^{3+}	100
			73.47	Pt^{2+}	20.4			
			76.55	Pt^{4+}	11.4			
[Pt(5wt%)Fe(2.5wt%)/CN-P]-N_2	0.34	0.75	71.87	Pt^o	69.1	707.37	Fe^o	59.7
			73.26	Pt^{2+}	17.5	709.35	Fe^{2+}	25.4
			75.80	Pt^{4+}	13.5	711.97	Fe^{3+}	14.9
Pt(5wt%)/CV	0.74	–	71.73	Pt^o	64.8	–	–	–
			73.22	Pt^{2+}	17.8			
			76.41	Pt^{4+}	17.5			
Pt(5wt%)Fe(0.35wt%)/CV	0.76	0.25	71.83	Pt^o	67.5	707.20	Fe^o	49.2
			73.56	Pt^{2+}	13.7	709.06	Fe^{2+}	27.0
			76.01	Pt^{4+}	18.9	711.14	Fe^{3+}	23.8
Pt(5wt%)Fe(2.5wt%)/CV	0.63	0.52	71.94	Pt^o	67.3	707.39	Fe^o	50.4
			73.22	Pt^{2+}	17.4	709.32	Fe^{2+}	32.5
			75.69	Pt^{4+}	15.3	711.47	Fe^{3+}	17.1
[Pt(5wt%)Fe(2.5wt%)/CV]-N_2	0.50	0.48	71.89	Pt^o	67.0	707.34	Fe^o	53.4
			73.27	Pt^{2+}	17.7	709.27	Fe^{2+}	31.3
			76.62	Pt^{4+}	15.3	711.79	Fe^{3+}	15.3

Table 6
XPS results of the PtSn catalysts series supported on CN-P and CV.

Catalyst	Atomic ratio		Pt $4f_{7/2}$ level			Sn $3d_{5/2}$ level		
	Pt/C	Sn/Pt	BE (eV)	Species	%	BE (eV)	Species	%
Pt(5wt%)/CN-P	0.60	–	71.67	Pt^o	63.61	–	–	
			73.06	Pt^{2+}	23.61			
			75.95	Pt^{4+}	12.77			
Pt(5wt%)Sn(0.5wt%)/CN-P	0.68	0.49	71.63	Pt^o	76.74	485.39	Sn^o	87.59
			73.42	Pt^{2+}	13.90	487.35	$Sn^{2+/4+}$	12.41
			76.69	Pt^{4+}	9.35			
Pt(5wt%)Sn(1wt%)/CN-P	0.56	1.57	72.05	Pt^o	82.29	485.52	Sn^o	87.02
			73.44	Pt^{2+}	8.45	487.45	$Sn^{2+/4+}$	12.98
			75.10	Pt^{4+}	9.27			
[Pt(5wt%)Sn(1wt%)/CN-P]-N_2	0.37	1.66	71.82	Pt^o	82.31	485.62	Sn^o	89.50
			73.23	Pt^{2+}	10.56	487.85	$Sn^{2+/4+}$	10.50
			74.64	Pt^{4+}	7.12			
Pt(5wt%)/CV	0.74	–	71.73	Pt^o	64.76	–	–	–
			73.22	Pt^{2+}	17.80			
			76.41	Pt^{4+}	17.45			
Pt(5wt%)Sn(1wt%)/CV	0.61	0.66	71.85	Pt^o	73.72	485.51	Sn^o	86.19
			73.29	Pt^{2+}	16.72	487.55	$Sn^{2+/4+}$	13.81
			75.30	Pt^{4+}	9.48			
Pt(5wt%)Sn(3wt%)/CV	0.57	1.48	72.01	Pt^o	82.43	485.43	Sn^o	87.38
			73.45	Pt^{2+}	13.43	487.14	$Sn^{2+/4+}$	12.62
			75.13	Pt^{4+}	4.15			
[Pt(5wt%)Sn(3wt%)/CV]-N_2	0.48	1.39	72.02	Pt^o	83.11	485.46	Sn^o	87.93
			73.42	Pt^{2+}	13.33	487.25	$Sn^{2+/4+}$	12.07
			74.91	Pt^{4+}	3.55			
Sn(3wt%)/CV	–	–	–	–	–	485.82	Sn^o	11.08
						488.36	$Sn^{2+/4+}$	88.92

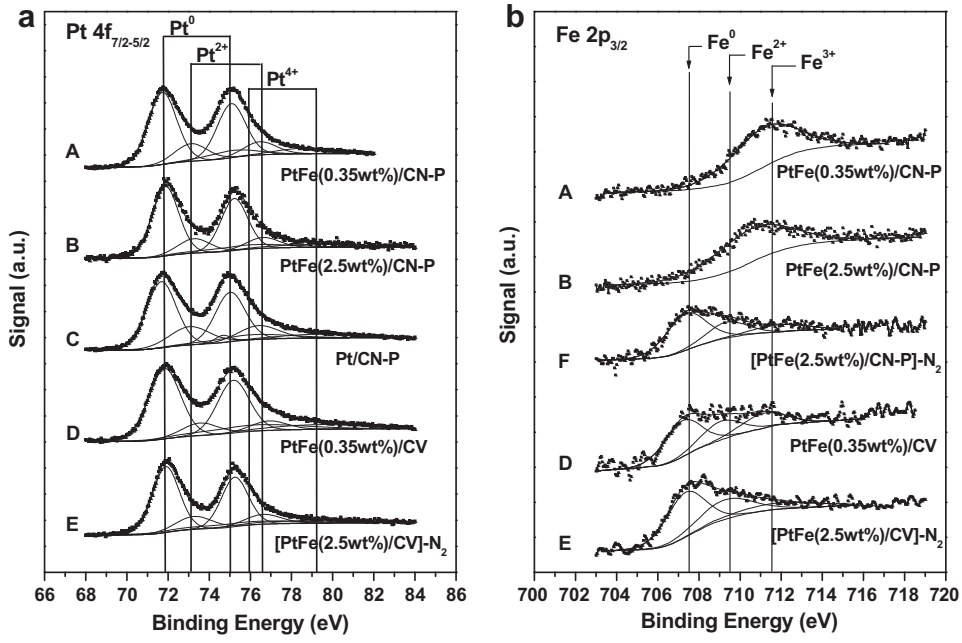

Fig. 3. Pt and Fe XPS profiles for PtFe catalytic series. (A) Pt 4f level and (B) Fe 2p level.

The XPS data of the PtSn catalysts series are quite different. From the deconvolution of the Sn $3d_{5/2}$ XPS spectra in all the catalysts, two peaks were obtained: one at low binding energy (about 485.4–485.6 eV) and other at about 487.2–487.8 eV. The first peak was assigned to zerovalent Sn, while the second one was attributed to oxidized species of $Sn^{2+/4+}$ since according to the literature, Sn^{2+} and Sn^{4+} cannot be discriminated because their binding energies are very similar [32,34,81] (see Fig. 4). From results displayed in Table 6, it can be observed that the addition of Sn to Pt increases the reducibility of Pt in both series. Besides, the percentage of reduced Pt in PtSn bimetallic catalysts increases with the Sn content increases, reaching values of about 82–83%. Regarding this fact, it must be pointed out that when impregnating, platinum could become reduced from Pt^{4+} in the metallic precursor to Pt^o and Pt^{2+} in the dried catalyst [2,17,32,64,65]. In this sense, we have reported that this Pt precursor is practically reduced to Pt^{2+} species over

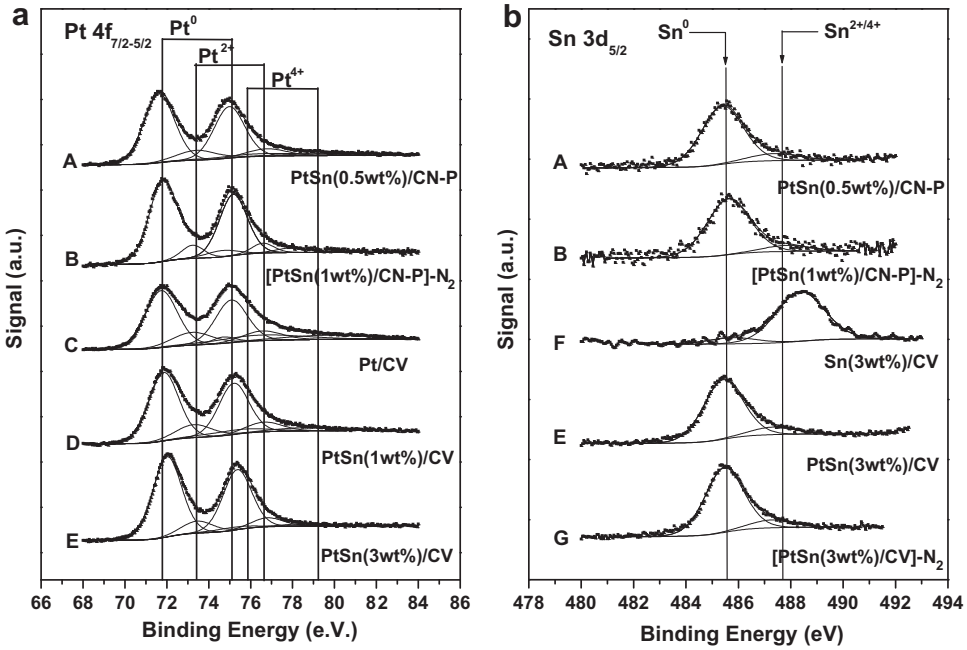

Fig. 4. Pt and Sn XPS profiles for PtSn catalytic series. (A) Pt 4f level and (B) Sn 3d level.

carbon nanotubes [55]. It could be also partially or totally reduced on carbon Vulcan, since the surface of this support was not modified by acid treatment, and it could have specific sites in the structure of the carbon basal planes to reduce the Pt^{4+} of the precursor during impregnation step [10,82]. It must be noted that the redox reaction could involve the oxidation of carbon support and also in this case the oxidation of Sn^{2+} from the Sn precursor to Sn^{4+} [32,12,13]. Thus, a certain amount of Pt could be reduced to Pt^{o} or partially to Pt^{2+} during impregnation step. If the reduction is Pt^{4+} to Pt^{2+}, this last species could be reduced easier than Pt^{4+} to Pt^{0} under hydrogen flow. In both cases, this fraction of Pt partial or totally reduced from the redox reaction of Sn could contribute to the higher percentage of metallic Pt found in these catalysts. On the other hand, it must be noted that the reduction of Sn^{4+} species to zerovalent state under hydrogen flow is expected to be more difficult. However, surprisingly, it was found a very high amount of Sn^{o} (86–90% for Sn loading from 0.5 to 3 wt%) in all the PtSn bimetallic catalysts of both series after reduction step (see Fig. 4 and Table 6). Since both supports present a certain amount of weak acid surface groups (according TPD results) which could be not very adequated to anchor the ionic species [1,12,13], a possible explanation of this effect could be that the $Sn^{2+/4+}$ species would have scarce affinity to be deposited on the support, thus prevailing the metal–metal interactions after the reduction step. In this sense, it must be noted that when the Sn precursor was impregnated alone on the support and treated with hydrogen at the same reduction temperature of the catalysts, very low Sn^{o}/Sn^{ionic} ratio (0.11) was found (see Fig. 4 and Table 6). Besides, it must be noted that the BE of the ionic fraction in the Sn(3wt%)/CV sample is shifted toward higher values than those of the bimetallic samples. This species were assigned to the presence of chlorinated tin species in the support, as it was suggested in the literature for other supports [83]. Regarding this fact, it must be noted that chlorinated and oxidized species could have a significative difference in the oxidation–reduction potentials on the support graphytic materials to prepare the catalysts. So, thus, it seems evident that a small fraction of Sn could form oxidized species from the reduction of Pt, thus contributing to the higher percentage of Pt^{o} species in PtSn bimetallic catalysts than the corresponding monometallic one, but also, in presence the Pt, chlorinated tin species would be easily reduced under hydrogen flow. Thus, the high percentage of Sn reduction is probably caused both by the support and the selected reduction method. Besides, this Sn reduction opens the possibility of the PtSn alloy formation. In this sense, the shift of the Pt binding energies toward slightly higher values than those observed in the monometallic sample could arise from alloy formation. Regarding this fact, it was reported in the literature high-resolution photoelectron spectroscopy results on well-defined PtSn alloys which show that Sn induces a shift in the surface component of the Pt 4f to higher BE compared to the BE of nonalloyed Pt surface [84]. Moreover, the BE value reported for the Sn $3d_{5/2}$ peak corresponding to non-supported PtSn alloys of 484.8 eV [85] is in agreement with our results. With regards to the Pt/C and Sn/Pt surface molar ratios in these series, it was found that Pt/C ratio decreases as the Sn content increases, at the same time that Sn/Pt ratio increases to values slightly higher than 1, thus indicating that there exists a certain surface enrichment in Sn. These results would be also indicating that Sn could geometrically modify the metallic phase by dilution and/or blocking effects with the presence of different Sn species (ionic, alloy or reduced). These effects seem to be more marked on CN-P support. In fact, it must be noted that the highest percentage of Pt reduction and the strongest change in Pt/C and Sn/Pt ratios are reached with different Sn loadings on both support, this being lower on CN-P support.

3.3. Characterization results discussion

From characterization results of the metallic phase, it could be concluded that both the support and the addition of a second metal have an important role in the preparation of the catalysts for selective hydrogenation. The second metal modifies the structure of the Pt particles, but different effects, such as dilution, blocking, or alloy formation, prevail in each catalytic series according to the support (carbon Vulcan or nanotubes) and the promoter (Fe or Sn) used for

prepare the catalysts. In this sense, some conclusions must be pointed out:

(i) The specific activities of the monometallic catalysts in both test reactions are lower for the Pt catalyst supported on carbon Vulcan than for Pt/CN-P. Since the monometallic catalysts have the same Pt loading (5%) and according to the H_2 chemisorption data, a similar Pt dispersion (29.8% and 27.2% for Pt/CN-P and Pt/CV respectively), this result would be related to a support effect due to the existence of a different accessibility of the reactants to the active sites, i.e., a lower steric restriction in the support would be present in catalysts supported on carbon nanotubes, in agreement with the properties reported in the literature for this new type of nanostructured support [46].

(ii) A different PtFe bimetallic phase is formed on carbon Vulcan in comparison with that on carbon nanotubes. In this sense, TPR results showed that Pt and Fe would have a better interaction on CV support, XPS results showed that there is a fraction of reduced Fe on CV, and Ea_{CH} measurements from CHD test reaction indicated that a higher electronic modification in PtFe catalysts supported on carbon Vulcan than on carbon nanotubes takes place. All the results are in agreement with the assumption that it would be a certain fraction of Fe forming alloy phases with Pt on CV, which does not appear on CN-P support. In order to interpret this aspect, two kinds of electron transfer mechanisms should be considered on these graphitic carbons, one from the support to the active metal and another one from promoter to Pt. Thus, since carbon nanotubes have a peculiar three-dimensional nanoscale structure with graphene layers deviated from planarity, a transfer of electronic density from the support to Pt particles could be favored [46,47,50,51], in addition to a good stabilization of ionic Fe particles on the support as it was reported in the literature [47,56,86,87]. On the contrary, on carbon Vulcan the deposition of metallic particles could take place preferentially at the edges of the basal plane structures in which functional groups exist. These functional groups could act as anchoring sites and/or hinder the electron transfer from support to Pt, but also, the ionic Fe particles could be less stabilized on the support. In this way, an electron transfer from promoter to Pt could be favored on carbon Vulcan with probable alloy formation when bimetallic catalysts prepared on carbon Vulcan are compared with those supported on carbon nanotubes.

(iii) For PtSn catalytic series supported on CN-P and CV supports it was observed a stronger modification of the metallic phase than for PtFe bimetallic series. In this sense, it must be noted that there is a sharp increase in the Ea_{CH} values together with a higher diminution of the CHD and CPH rates in the PtSn catalytic series than in the PtFe catalytic ones. These results can be related with those found from TPR and XPS experiments: TPR results showed a higher Pt–Sn interaction than Pt–Fe, and XPS results evidenced a very high fraction of Sn species in zerovalent state in all catalysts supported on both supports. Thus, all these characterization results would be indicating a strong electronic modification of metallic phase and an important fraction of Pt–Sn alloyed species that could be present together with a small fraction of ionic and reduced Sn species. Again, the influence of the support over the different metal–metal and metal–support interactions could help to explain these results. In this sense, it must be noted that one of the advantages of the carbon supports with respect to conventional oxidic supports (like alumina and silica) is the easy reducibility of the metals due to the relative inert character of the surface would avoid strong promoter-support interactions [1,3,11] and would ease the metal–metal interaction and the formation of alloy phases [1]. However, in spite of these facts, it must be noted that most of studies with bimetallic catalysts over carbons show that although a certain fraction of the promoter could be reduced, this fraction is never higher than the corresponding ionic one [12,13,16,18,28,29,31–36,88]. Thus, in comparison with the data found in the bibliography, our results show that the degree of reducibility of the second metal is strongly dependent on the type of carbon and the nature of the promoter used to prepare the bimetallic catalyst. In this sense, Fe has a quite typic behavior to modify the active phase by introducing different species both over the support surface and metallic phase, while surprisingly Sn has a quite different behavior due to the important co-reduction of this promoter with Pt over these carbonaceous materials. The poor interaction of Sn with the carbonaceous supports could be understood considering that carbons have different anchoring sites for metals than oxidic supports and other carbon types (like unsaturated valences, basic sites of the support and heteroatoms of different functional groups). Besides, the better stabilization of Fe than Sn on CN-P and CV supports, could be understood taken into account that Fe is a d-transition metal whose donor–acceptor electronic properties are different from the corresponding binding properties of a s,p element, like Sn.

(iv) In addition to the above-mentioned results, other important difference regarding the role of Fe and Sn as a promoter can be observed from the range of loading studied for each one (see Table 1). The results also show that it is necessary a high Fe/Pt bulk molar ratio ($\gg 1$) to modify the Pt metallic phase in an important way, probably due to the promoter-support interaction is favored in this condition. On the contrary, the results from PtSn catalytic series show that a very low amount of Sn (Sn/Pt bulk molar ratio $\ll 1$) is enough to significantly modify the active phase (this effect being in turn more evident on CN-P support), and thus showing that when Sn is used as a promoter on the studied carbonaceous materials, the metal–metal interaction prevails.

3.4. Citral hydrogenation

Citral (3,7-dimethyl-2,6-octadienal) was selected as reaction substrate in the studies of selective hydrogenation. Fig. 5 shows the scheme of the citral hydrogenation reaction. Citral has three groups able to be hydrogenated; it contains both an isolated and a conjugated double bond, as well as a carbonyl group. So, the non-selective hydrogenation of citral results in a parallel and consecutive reduction of the two functional groups until to obtain the product of the complete hydrogenation (3,7-dimetiloctenol). Thus, unsaturated alcohols (geraniol and nerol) and partially unsaturated aldehydes (citronellal and 3,7-dimetil-2-octenal) can be formed as primary parallel products of monohydrogenation, and 3,7-dimetil-2-octenol, citronellol and 3,7-dimetiloctenal can be formed in a second hydrogenation step. It must be noted that aliphatic aldehydes such as citronellal and dihydrocitronellal can react with an alcoholic solvent to form acetals. Besides, other side reactions, such as decarbonylation, isomerization, hydrogenolysis, or cyclization of citronellal, can lead to different by-products. These side reactions can be controlled by the proper choice of the metal precursor and the support, and the hydrophobic character and stereochemistry of the solvent [89,90]. So, in this work, the hydrogenation was performed in 2-propanol (a hindered alcohol) in order to avoid by-product formation from side reactions of the solvent [33,89,90].

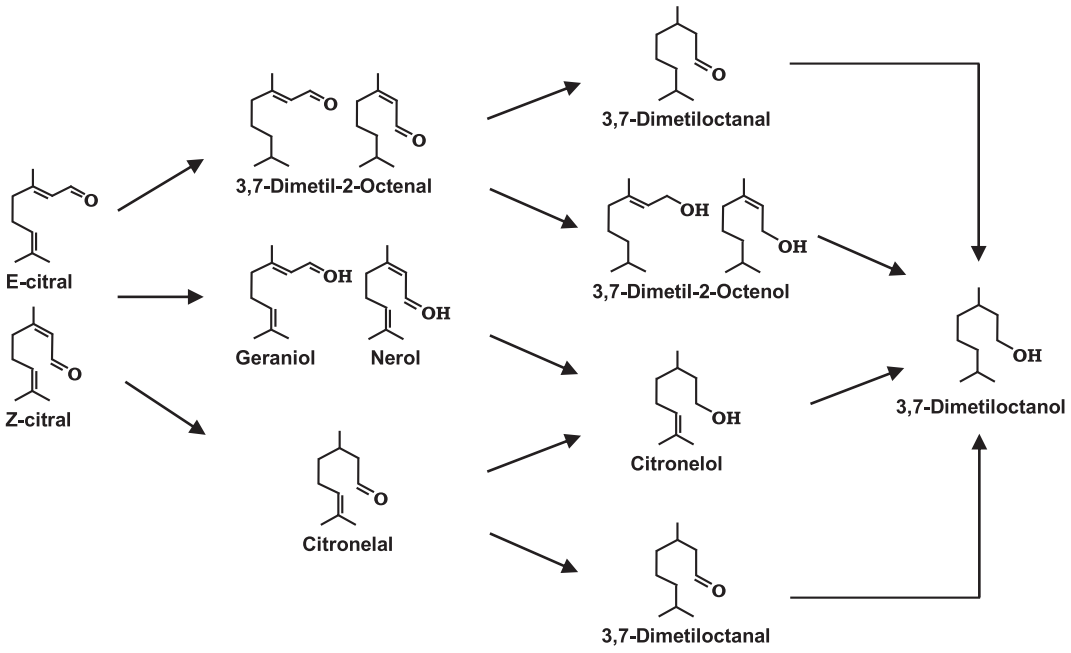

Fig. 5. The hydrogenation pathways of citral.

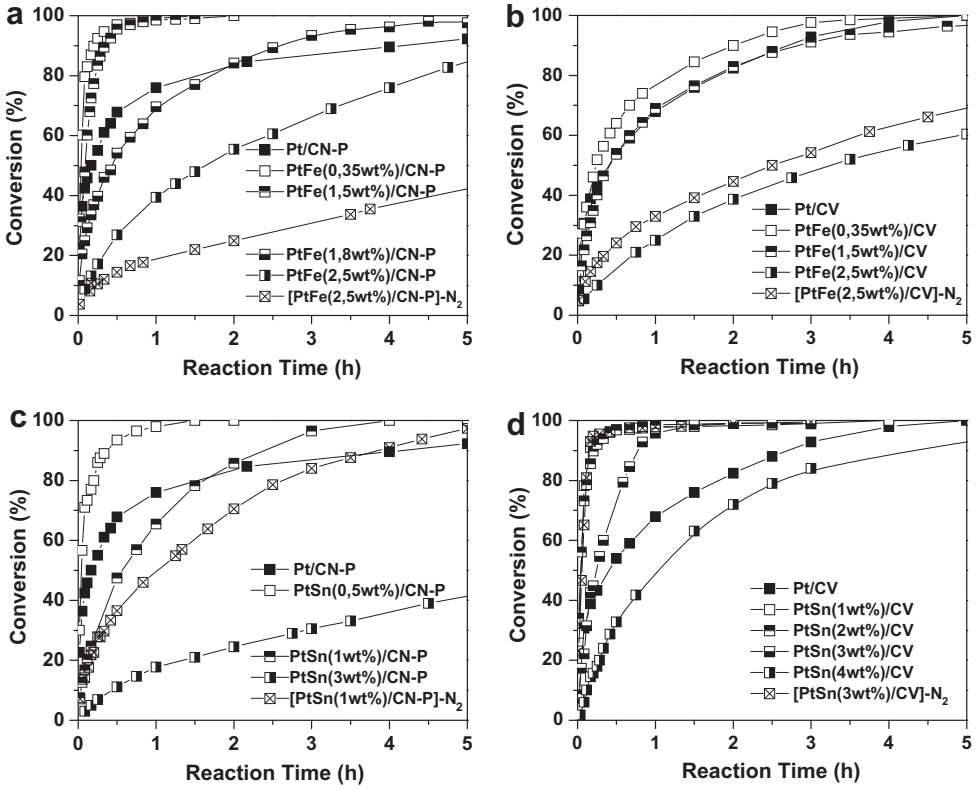

Fig. 6. Citral conversion as a function of the reaction time for the different bimetallic catalytic series. (A) PtFe/CN-P, (B) PtFe/CV, (C) PtSn/CN-P, and (D) PtSn/CV.

Fig. 6 shows the results of the citral conversion to all products as a function of the reaction time for each catalyst series: PtFe/CN-P and PtFe/CV, PtSn/CN-P, and PtSn/CV. It must be noted that in order to show a better detail of the behavior of the catalysts at low reaction time, in all the curves, the activity was plotted up to a same reaction time (5 h). Fig. 7 displays the relative activity as a function of the Fe or Sn content for the corresponding catalytic series. The relative activity was defined as $\theta_{Pt}/\theta_{Pt-Promoter}$ ratio taking into account the required reaction times (θ) to reach the 95% of citral conversion for each one of the catalysts. As it can be seen in Fig. 6, the activities of the bimetallic catalysts supported both on carbon Vulcan and carbon nanotubes with low loading of Fe and Sn are higher than those of the corresponding monometallic ones. However, this effect is much more marked for PtFe and PtSn

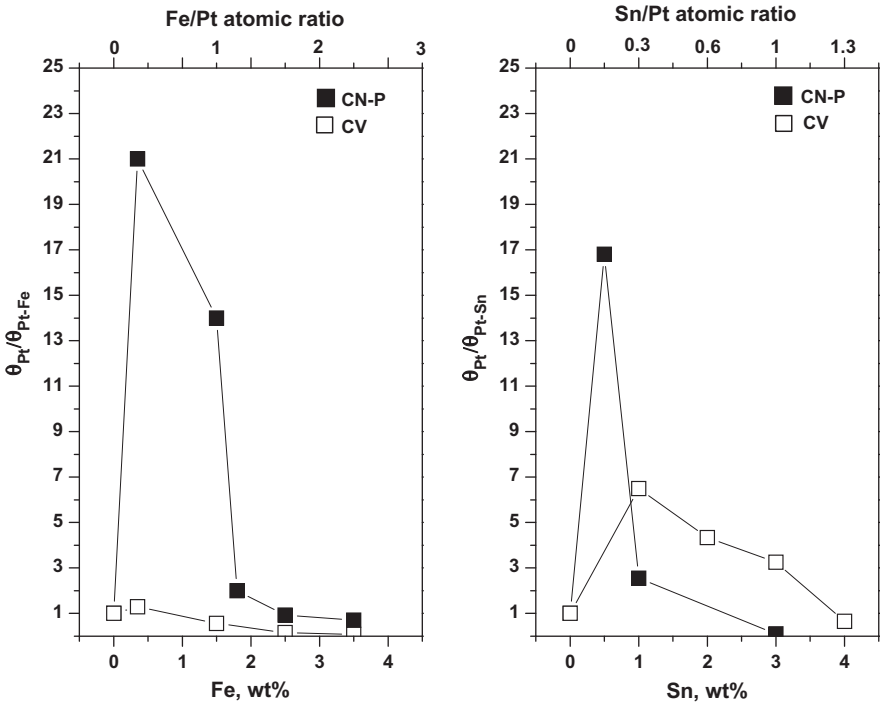

Fig. 7. Relative activity ($\theta_{Pt}/\theta_{Pt-Promoter}$) in citral hydrogenation versus Fe and Sn content for the different bimetallic catalytic series supported on CN-P and CV.

catalysts supported on CN-P. As it can be observed in Fig. 7, the relative activities for the lowest loading of the promoter in these catalytic series were more than 10 times higher than that corresponding to the monometallic one. Besides, it was observed in Figs. 6 and 7 that for other promoter loadings in bimetallic catalysts supported both on CV and CN-P, the higher Fe or Sn contents, the less active the catalysts; these relative activities being for catalysts with the highest promoter loading very approximately 10 times lower than the corresponding of the monometallic ones. On the other hand, from results displayed in Fig. 6, other effects can be observed. First, it must be noted that those bimetallic catalysts with Fe or Sn supported on CV and treated with N_2 show a higher activity than that corresponding to the parent bimetallic catalyst without any treatment, while PtFe or PtSn bimetallic catalysts supported on CN-P and treated with N_2 show an opposite behavior. In this sense, the Pt/C and Promoter/Pt surface molar ratios found from XPS results could help to explain these results. On CV support, the Pt/C and Promoter/Pt ratios slightly decrease for both bimetallic series when the catalysts are submitted to the thermal treatment with N_2. On CN-P support, the Pt/C ratios for both bimetallic series decrease more significantly than those corresponding on CV support, while Fe/Pt and Sn/Pt ratios practically remain constant after the thermal treatment. These changes would evidence a modification of bimetallic phases by the thermal treatment which produce a higher amount of exposed Pt sites on CV than CN-P support together with a higher relative amount of sites provided by the promoter which could increase the activity of certain hydrogenation reactions (see below), thus explaining the high global activity in the catalysts supported on CV and treated with nitrogen. Second, it can be also observed that the curve corresponding to Pt/CN-P catalyst shows different behaviors with respect to that of the monometallic catalyst supported on CV. The initial reaction rate of Pt/CN-P catalyst is higher than the corresponding to Pt/CV one (0.0090 and 0.0042 mol L^{-1} min^{-1}, respectively), but the activity of Pt/CN-P catalyst shows a flattening after 0.5 h of reaction time, and then, it significantly decreases at higher reaction time. These different behaviors could be attributed both to an effect of the support due to different structure of the carbons and the presence of different surface acid oxygenated groups on CN-P and CV supports which together with the active metal could catalyze in different extension the above-mentioned side reactions in competition with the desired hydrogenation ones [55]. The effect of the support nature over the selectivity for monometallic catalysts supported both on CN-P and CV will be analyzed below.

In order to understand the catalytic behavior in these series, the above-mentioned effects must be related with the characterization results and nature of the support. On the one hand, when Fe or Sn are added to Pt/CN-P or Pt/CV, a fraction of these metals, which are in the vicinity of Pt atoms, could selectively promote certain hydrogenation reactions [22,23], and other fraction probably could interact with surface acid groups of the support poisoning and inhibiting undesirable side reactions. In this way, both effects explain the increase in the relative activity at low promoter loading, but also, it must be taken into account that the higher the promoter content, the higher the dilution or blocking of the Pt metal by the promoter, and in consequence, it would be expected a lower activity when increasing promoter amounts are added to the Pt, as it was observed. On the other hand, additional effects must be taken into account to explain some differences regarding to relative activity found for PtFe or PtSn catalysts supported on CN-P or CV. Thus, the difference in term of relative activity changes between Pt catalysts with the addition of Fe on CN-P or CV supports must be attributed to oxidation state of Fe in these catalysts. According to XPS results, on CN-P support, Fe is present in an ionic state. This ionic Fe fraction in the corresponding catalyst with a low loading (PtFe(0.35wt%)/CN-P) inhibits side reactions and enhances the global hydrogenation rate with respect to that found for the parent Pt monometallic catalyst. On CV support, an important fraction of Fe is present in zerovalent state, even at low promoter content, probably forming alloyed phases. In this case, it was found in test reactions that PtFe alloys would have a certain catalytic activity, but this activity would be lower than the corresponding to the parent Pt catalyst. Besides, it was reported in the literature that alloy phases of PtFe, PtCo, and PtNi could be active in hydrogenation reactions [1,16,23,24,73,91–93]. So, the slight increase in the

relative activity for PtFe(0.35wt%)/CV could be due to the presence of the some fraction of PtFe alloy which would not change significantly the activity of the monometallic phase, although the inhibition of side reactions must not be discarded. Another important difference of activity can be observed in the PtSn series. When Sn is added to Pt supported on CN-P or CV, the change in the relative activity with the Sn loading seems to be more similar on both supports, showing a maximum at low Sn content. However, it must be noted that the PtSn/CN-P series show a Sn loading range narrower than for the PtSn/CV series where the activity is higher than that corresponding to the Pt parent catalyst. This effect would be showing that it is necessary only a small amount of Sn (which corresponds to very low Sn/Pt molar ratio) to promote hydrogenation reactions and inhibit side reactions probably due to a different surface exposure degree of metallic phase and different steric requirements on CN-P support with respect to CV one.

Since in all cases, the activity changes can be correlated with the promotion of certain hydrogenation reactions and the inhibition of side ones, the immediate consequence is the change in the selectivity of the different catalysts. Fig. 8 shows the selectivity values to different reaction products measured at three citral conversion levels (35%, 65%, and 95%) for the catalysts corresponding to PtFe and PtSn series supported on CN-P and CV supports. In order to highlight the selectivity toward the desirable products, Fig. 9 only shows the selectivity values to unsaturated alcohols for all the catalytic series. From these results, it can be observed that the monometallic Pt catalysts on both supports are not selective to unsaturated alcohols, but also that the selectivities toward the hydrogenation of conjugated double bond are decreased due to the formation of side products. In addition, it can be seen that Pt/CN-P catalyst is more selective to the products of mono and bi-hydrogenation than Pt/CV one, citronellal (CAL) being rapidly produced at the initial step of the reaction and then transformed in citronellol (COL). This fact would help to explain the different kinetic behaviors and the activity results found for both monometallic catalysts, since CN-P support has different surface oxygenated groups (according to the TPD results) than CV support and these groups could help to catalyze different side reactions. Besides, even though the Pt dispersion in Pt/CN-P and Pt/CV catalysts is similar (29.8% and 27.2%, respectively), a different accessibility to the active sites could exist due to the different steric structure of both supports, as it was above mentioned from characterization results.

It is also observed in Figs. 8 and 9 that bimetallic catalysts on both supports display a notorious higher selectivity to unsaturated alcohols than the corresponding monometallic ones, as it was expected from the promoter role of the second metal [38–40]. For PtFe bimetallic catalysts supported both on CN-P and CV, it can be observed that the higher the Fe loading added to Pt, the higher the selectivity to UA, while the selectivity toward side reactions significantly decreases for the lowest Fe loading and it becomes negligible for high loadings. Besides, it must be noted that the selectivities to CAL and COL are also increased for the lowest Fe content with respect to the corresponding monometallic catalysts, but for other Fe loadings, the higher the Fe content, the lower the selectivities to these hydrogenation products. Three important effects must be taken into account to explain these results. First, as it was above mentioned, ionic Fe species poison the acid sites on the support [47,55,87], thus inhibiting side reactions and contributing to a higher selectivity to UA in both bimetallic catalytic series. In this sense, it is logic to observe that there is a certain Fe loading to eliminate side reactions. The other two effects would be related to the action of Fe as a promoter. It is important to point out that the ionic Fe can bind and activate not only to the carbonyl group, but it can also form complexes with the double bond, thus promoting its hydrogenation [23,24]. However, it must be noted that the competition between C=O and C=C groups for the same site on PtFe catalysts can be suppressed in favor of C=O hydrogenation by steric factors of the substrate or the reaction medium [24]. On the other hand, Fe can form alloy with Pt, and it was reported that Fe in these alloyed phases has a slightly positive charge, thus creating polar bimetallic sites able to interact with the carbonyl group [23,24]. So, in the case of PtFe(0.35w%)/CN-P and PtFe(0.35w%)/CV catalysts, a small concentration of ionic Fe, which modifies the metallic Pt phase, could promote the hydrogenation of C=C and C=O groups. Besides, on CV support, the presence of an additional PtFe alloy phase in the PtFe(0.35w%)/CV catalyst could promote only the C=O hydrogenation, thus contributing to a higher selectivity to UA. Regarding other Fe content, when higher loadings of Fe are added to Pt on both supports, only an increase in the promotion effect to UA is observed, while the hydrogenation of CAL is decreased. This fact could be explained taking into account that the structure or adsorption mode could change with the total density of molecules competing for a given number of sites. In this sense, the adsorption of citral via the C=C bond would require more space (which would block other sites), a determinated structure of adsorption sites, and major availability of accessible H atoms on the metal surface than the adsorption via the C=O bond. These effects would also explain why the selectivity to UA in catalysts with high Fe loadings does not significantly decrease with the progress of the reaction (such as it was observed at low loading after 65% citral conversion) since the unsaturated alcohols would be more difficult to hydrogenate on these bimetallic phases.

In the case of the PtSn catalytic series, other effects must be considered to explain the selectivity results. Figs. 8 and 9 show that for PtSn bimetallic catalysts supported on both supports, the selectivity to UA is modified in an important degree with the addition of low Sn loadings to Pt, reaching a 70–80% for the lowest Sn loadings at 65% citral conversion. Besides, the selectivity to UA increases from about 70% for PtSn(0.5wt%)/CN-P catalyst to about 90% for PtSn(1wt%)/CN-P catalyst, remaining practically unmodified with the progress of the reaction both in the last catalyst and those catalysts with higher Sn loadings. In the case of PtSn catalysts supported on CV support, the selectivity to UA slightly increases as the Sn loading increases. However, it can also be observed that there is an improvement in the selectivity to UA at 95% citral conversion when increasing Sn amounts are added to Pt. These results would be indicating a stronger promotion effect of Sn at low loadings than Fe. It is known that according to the order established by experiments from the different works in the literature [23], Sn shows a stronger effect on the selectivity to UA in the hydrogenation of α,β-unsaturated aldehydes than Fe. As it was reported in those studies, this fact was explained as Sn is a s,p element which remains mainly in ionic state under the catalyst preparation conditions and it does not bind the olefinic group. However, the results obtained with Sn in this work differ respect to those previously reported due to a different bimetallic phase is formed. The results are surprising since it was found by XPS experiments that Sn is almost completely reduced to metallic state for all the loadings studied. So, as a consequence of this fact, it should be noted that the small fraction of Sn (about 10–12% of the corresponding Sn loading) that remains in ionic state should have two roles to enhance the selectivity to UA. According to the literature, one of them would be the inhibition of side reactions by poisoning of acid sites of the support, and the other one would be the proper action as a promoter to active the carbonyl group [34,55]. In this sense, theoretical predictions supported by experimental results show that the selectivity to C=O versus C=C hydrogenation in an α,β-unsaturated aldehyde is mainly determined by the extent of the activation of the C=O group which can be achieved by the promotion of the metallic catalyst by an ionic compound with a positively charged

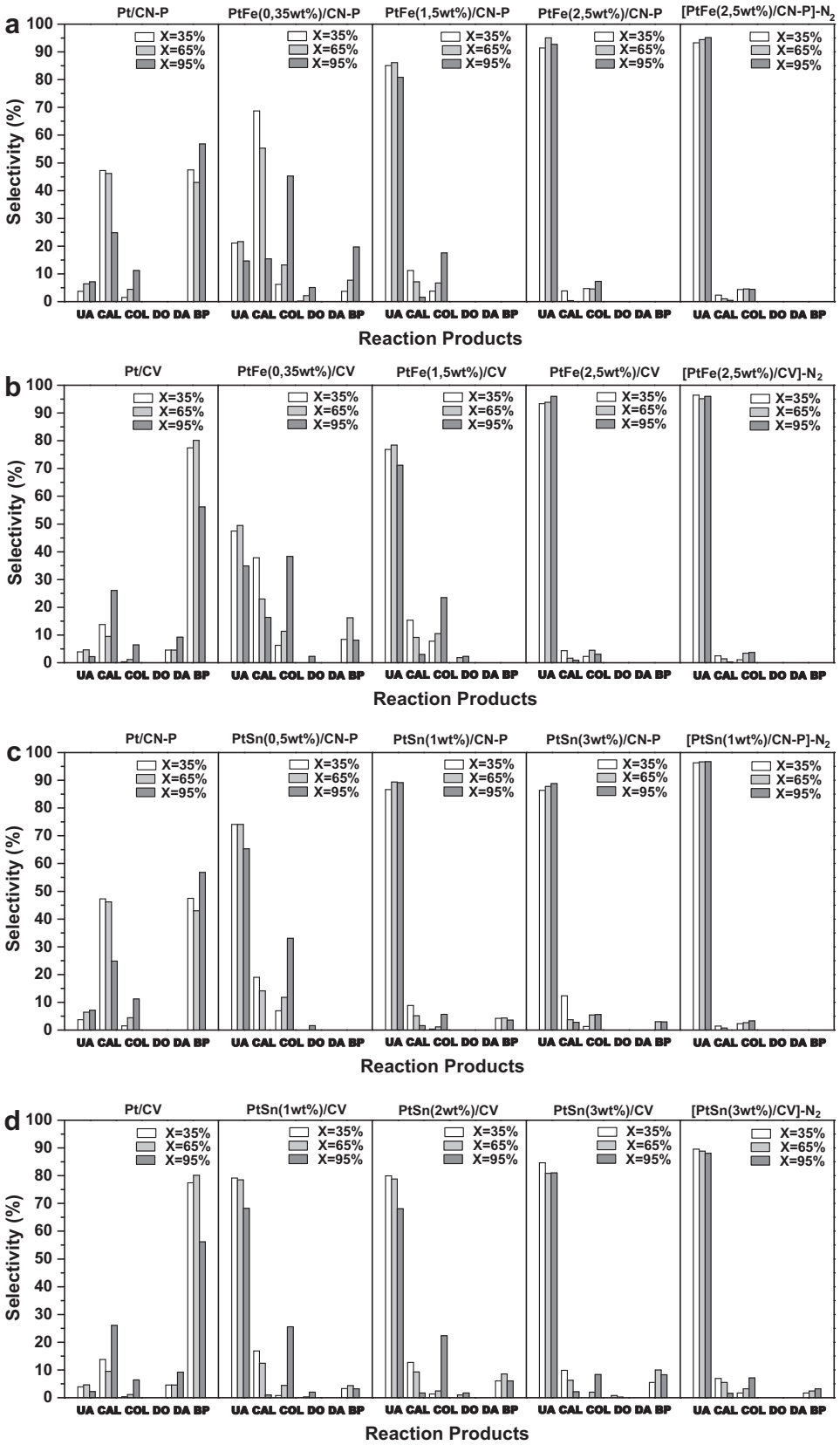

Fig. 8. Selectivities to different products measured at different citral conversión levels of 35%, 65% and 95% for the different bimetallic catalytic series: (A) PtFe/CN-P, (B) PtFe/CV, (C) PtSn/CN-P, and (D) PtSn/CV. UA: unsaturated alcohol (geraniol and nerol), CAL: citronellal, COL: citronellol, DO: 3,7-dimethyloctanol, DA: 3,7-dimetiloctanal, BP: byproducts.

cationic site able to act as Lewis-acid site [18,23]. However, as the C=O activation has been found to be dependent on the promoter loading, these fundaments would not explain correctly the selectivity changes found in this work. So, in this work, we would like

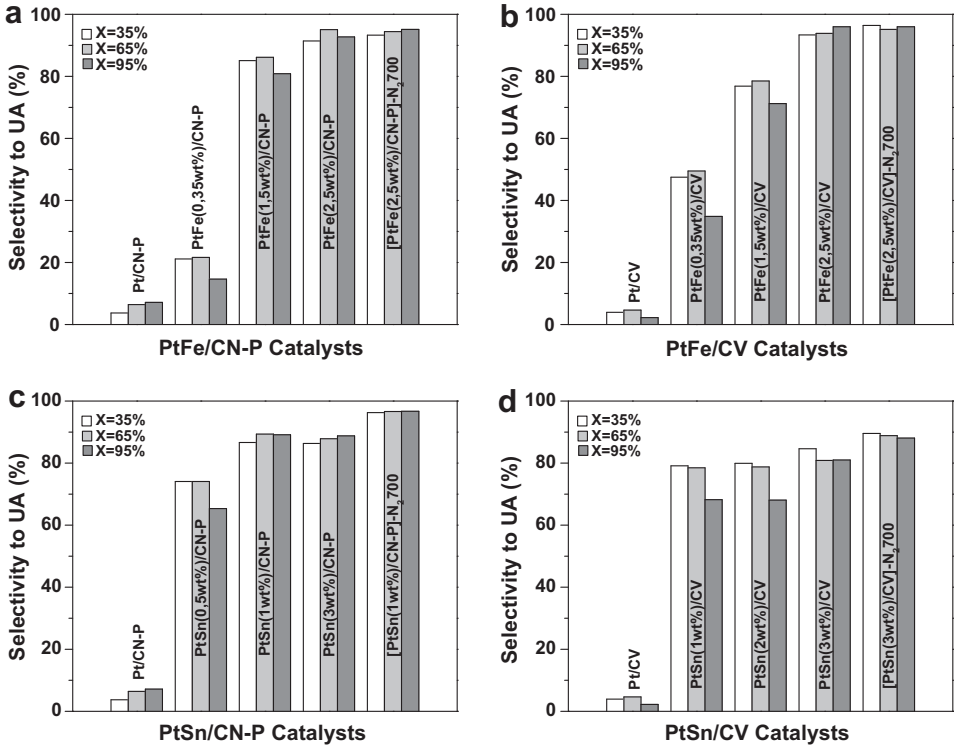

Fig. 9. Selectivities to UA measured at different citral conversión levels of 35%, 65% and 95% for the different bimetallic catalytic series: (A) PtFe/CN-P, (B) PtFe/CV, (C) PtSn/CN-P, and (D) PtSn/CV.

to propose a different fundament to explain the important improvement in the selectivity to UA when PtSn catalysts are used in the citral selective hydrogenation.

Since the platinum–tin interaction in the final catalyst seems to be of great importance in obtaining a high selectivity to UA, special attention was taken into account about the presence of alloy phases. From characterization results, it was emphasized that an important fraction of Pt–Sn alloyed species could be present modifying the metallic phase. However, the presence of a certain fraction of reduced Sn in nearby contact with Pt should not be discarded. In both cases (Sn^o alone or PtSn alloys), the Sn would contribute to a dilution effect of Pt by these species, which in addition to the presence of oxidized species could be responsible for the selective polarization of the carbonyl group. However, it was observed the presence of very low amounts of ionic species in all catalysts (the best example being about 0.05 wt% or a Sn/Pt molar ratio of 0.015 in the PtSn(0.5wt%)/CN-P catalyst), and according to the literature, it is known that the dilution of an active phase by a non-active metal would have little or no influence on the selectivity [22–24]. So, it seems that this dilution additional effect on the bimetallic phase would be not enough to explain the hydrogenation results. On the other hand, with respect to the metallic Sn, it must be also taken into account that Sn^o alone is catalytically inactive for the hydrogenation of double bonds [23], but it must be pointed out that the literature is less clear about the effect of alloy species on the hydrogenation [12,13,18,28,35,36,85,88,94,95]. Even when PtSn alloys formed in some catalyst systems for selective hydrogenation of α,β-unsaturated aldehydes have shown an improvement in the selectivity to UA [35,36], the origin of this effect has not been totally understood and several hypotheses exist, the most used being the one that involves the action of Sn as an inert. Besides, it must be point out that the literature refers to the existence of the alloyed fractions in lower proportion than those corresponding to oxidized species, and it is assumed that the main cause of the polarization of carbonyl group is the presence of oxidized species in the catalytic surface. In this paper, it is proposed that the PtSn alloyed species would be active and mainly responsible for the enhancement observed toward the hydrogenation of carbonyl group in PtSn/CN-P and PtSn/CV catalysts.

Regarding the promotion mechanism of carbonyl group on PtSn alloys, it is important to mention studies carried out by Delbecq and Sautet [94]. These authors studied the adsorption of the α,β-unsaturated aldehydes by means of density functional calculations (DFT) on well-defined Pt–Sn alloys and Pt(111) surfaces. Two interesting conclusions were found. First, according to the characterization of the alloys, it was observed that a charge transfer from Sn to Pt occurs in agreement with the relative electronegativities of the atoms (2.2 and 1.8 for Pt and Sn, respectively, according to Pauling's scale). This transfer induces some polarity on the alloy leading to positively charged Sn atoms which could act as Lewis-acid sites. Second, it was observed that for the most stable adsorption structures of α,β-unsaturated aldehydes, the adsorption energy is smaller on the alloys than on platinum, but it was also observed that on alloys, there is an enhancement of the relative stability of adsorption structures which leads to the hydrogenation of carbonyl group. Besides, the second hydrogenation (hydrogenation of the formed unsaturated alcohol) does not take place on the alloy as it does on platinum, due to that UA is adsorbed in a vertical mode and no activation of C=C occurs. Thus, even though experiments have been carried out on non-supported catalysts, these observations could help to explain certainly our results, thus indicating that polar bimetallic sites created by alloyed species could replace oxidized Sn species in their function as promoter. Fig. 10 shows a scheme of the proposed model for PtSn catalysts in comparison with that corresponding to PtFe samples.

Finally, from results displayed in Fig. 7, it can be also observed the selectivity results for bimetallic catalysts with high promoter loading and treated with N_2 at high temperature. It must be noted that

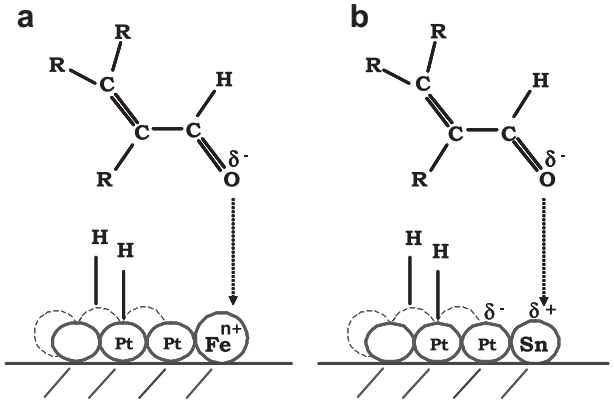

Fig. 10. Schemes of the proposed models for the promotion of C=O group in PtFe (A) and PtSn (B) catalysts.

PtFe bimetallic catalysts supported on CN-P and CV supports with the above-mentioned thermal treatment do not show an important change in the selectivity values, while PtSn bimetallic catalysts show an increase in the selectivity to UA, this effect being more marked in PtSn series supported on CN-P support. These results can be explained taken into account that Fe would be better anchored on the support than Sn, as it was above mentioned. So, in these cases, the sinterization during the thermal treatment would be more hindered due to the high Fe loading on the support which does not allow the desorption of functional groups [10,55]. For Sn, on the other hand, the sintering could be easier, and it would be more effective on supports with certain surface oxygenated groups able to be desorbed to high temperature, the last effect explaining why the sinterization on CN-P is higher than on CV support. In this sense, it must be noted that it was obtained the best selectivity to UA (about 97–98%) and a good activity for the [PtSn(1wt%)/CN-P]N_2 catalyst, which presents an appropriate equilibrium between the particle size, interaction of the particles with the support and Sn promoter amount.

Summarizing, the catalytic performance in the citral hydrogenation can be adequately correlated with the characteristics of the metallic phase: presence of different promoter species, the reducibility of Pt and promoter and the interaction degree of these metals that takes place in the different catalysts. In this sense, the effect of the carbonaceous material used as support on the preparation of the bimetallic catalysts has a fundamental role in the formation of different Pt–promoter phases suitable for selective hydrogenation. According to the literature, activated carbons of large surface area have been widely used to prepare bimetallic catalysts for selective hydrogenation, and most of the works derived from these studies report important changes in relation to the selectivity of the reaction. However, none of these works report selectivities to UA as high as 98%. We used two different carbon types to prepare catalysts: carbon nanotubes, whose exceptional physicochemical properties make them interesting targets for the investigation in selective hydrogenation, and carbon Vulcan which is a non-conventional support to prepare catalysts for hydrogenation. In this sense, our work reports new and important studies about preparation and characterization of PtFe and PtSn catalysts supported over two different carbons and their performances in the selective hydrogenation of α,β-unsaturated aldehydes to unsaturated alcohols, citral being selected as reaction substrate and reaching very high selectivities to geraniol and nerol.

4. Conclusions

The results obtained in this study can be summarized as follows:

- The addition of a second metal has an important role in the preparation of the catalysts for selective hydrogenation. The second metal modifies the structure of the Pt particles in a different way according to the support (carbon Vulcan or nanotubes) and the promoter (Fe or Sn) used for prepare the bimetallic catalysts.
- For PtFe catalysts supported on both supports, Fe ionic species prevail on the bimetallic surfaces producing mainly a geometric effect. For both bimetallic series, it was found that it is necessary to add Fe amounts in a Fe/Pt molar ratio higher than 1 to obtain a strong modification of the metallic phase. As it was expected from the correlation of the characteristics of these bimetallic structures with the performance of the catalysts in the citral selective hydrogenation, the higher the modification of the metallic phase, the higher the selectivity to UA. The highest selectivity to UA (about 90–95% for both series) was achieved for a Fe loading of 2.5 wt%. In these catalysts, a main fraction of ionic species together with the dilution effect would explain the selectivity changes in the bimetallic catalysts with respect to the corresponding monometallic ones. However, it was observed a lower activity in catalysts supported on Vulcan carbon than those supported on nanotubes carbon, this being inverted after the thermal treatment with N_2 at high temperature, so an effect of the support takes place.
- For PtSn catalysts supported on both supports, reduced Sn species prevail on the bimetallic surfaces producing mainly an electronic effect. In this case, for PtSn bimetallic series supported on CN-P it was found that it is enough to add Sn in a Sn/Pt molar ratio lower than 1 to obtain a strong modification of the metallic phase, while for PtSn bimetallic catalyst supported on CV the best molar ratio was equal to 1 for the same purpose. Surprising results were obtained with these bimetallic phases in the citral selective hydrogenation. The highest selectivities to UA were nearby 80% for the PtSn(3wt%)/CV and 90% for the PtSn(1wt%)/CN-P catalysts. In these catalysts, a main fraction of alloyed PtSn species able to active the carbonyl group together with the dilution effects would be responsible of the selectivity changes in the bimetallic catalysts with respect to the corresponding monometallic ones. In the case of PtSn(1wt%)/CN-P catalyst the thermal treatment with N_2 significatively enhances the selectivity to UA toward values of 98% at 95% citral conversion, keeping a good activity in relation to that of the parent catalyst without any treatment. The last effect would be related to the formation of a more adequate bimetallic phase after sinterization on CN-P support than on the CV one.

Acknowledgments

Authors thanks to Miguel A. Torres and to María Fernanda Mori for the experimental assistance. This work was made with the financial support of ANPCYT and Universidad Nacional del Litoral (Project CAI+D) – Argentina.

References

[1] F. Rodríguez-Reinoso, Carbon 36 (1998) 159.
[2] A. Sepúlveda-Escribano, F. Coloma, F. Rodríguez-Reinoso, Appl. Catal. A: Gen. 173 (1998) 247.
[3] M.C. Román-Martínez, D. Cazorla-Amorós, A. Linares-Solano, C. Salinas-Martínez de Lecea, Curr. Top. Catal. 1 (1997) 17.
[4] C.N. Satterfield, Heterogeneous Catalysis in Practice, McGraw-Hill, New York, 1980.
[5] E. Auer, A. Freund, J. Pietsch, T. Tacke, Appl. Catal. A: Gen. 173 (1998) 259–271.
[6] M. Suzuki, Carbon 32 (1994) 577.
[7] P. Serp, M. Corrias, P. Kalck, Appl. Catal. A: Gen. 253 (2003) 337.
[8] P.M. Ajayan, Chem. Rev. 99 (1999) 1787F.
[9] H. Jüntgen, Fuel 65 (1986) 1436.

[10] F. Coloma, A. Sepúlveda-Escribano, J.L.G. Fierro, F. Rodríguez-Reinoso, Langmuir 10 (1994) 750.
[11] S.A. Stevenson, J.A. Dumesic, R.T.K. Baker, E. Ruckestein, Metal–Support Interactions in Catalysis, Sintering and Redispersion, Van Nostrand Reinhold Catalysis Series, Van Nostrand Reinhold, New York, 1987.
[12] F. Coloma, A. Sepúlveda-Escribano, J.L.G. Fierro, F. Rodríguez-Reinoso, Appl. Catal. A: Gen. 136 (1996) 231.
[13] F. Coloma, A. Sepúlveda-Escribano, J.L.G. Fierro, F. Rodríguez-Reinoso, Appl. Catal. A: Gen. 148 (1996) 63.
[14] H. Jung, P.L. Walter, M.A. Vannice, J. Catal. 75 (1982) 416.
[15] A. Guerrero-Ruíz, A. Sepúlveda-Escribano, I. Rodríguez-Ramos, Appl. Catal. A: Gen. 81 (1992) 81.
[16] M.C. Román-Martínez, D. Cazorla-Amorós, H. Yamashita, S. de Miguel, o.A. Scelza, Langmuir 16 (2000) 1123.
[17] M.C. Román-Martínez, D. Cazorla-Amorós, A. Linares-Solano, C. Salinas-Martínez de Lecea, H. Yamashita, M. Ampo, Carbon 33 (1995) 3.
[18] P. Mäki-Arvela, J. Hájek, T. Salmi, D.Yu. Murzin, Appl. Catal. A: Gen. 292 (2005) 1.
[19] P. Gallezot, A. Giroir-Fendler, D. Richard, in: W. Pascoe (Ed.), Catalysis of Organic Reactions, Marcel Dekker, New York, 1991, p. 1.
[20] F.V. Wells, M. Billot, Perfumery Technology, E. Horwood Publishers, Chichester, UK, 1981. p. 149.
[21] U.K. Singh, M.A. Vannice, J. Catal. 199 (2001) 73.
[22] V. Ponec, Appl. Catal. A: Gen. 149 (1997) 27.
[23] M. Englisch, V.S. Ranade, J.A. Lercher, J. Mol. Catal. A: Chem. 121 (1997) 69.
[24] T.B.L.W. Marinelli, S. Nabuurs, V. Ponec, J. Catal. 151 (1995) 431.
[25] P. Claus, Top. Catal. 5 (1998) 51.
[26] B. Bachiller-Baeza, A. Guerrero-Ruíz, P. Wang, I. Rodríguez-Reamos, J. Catal. 204 (2001) 450.
[27] N. Mahata, F. Goncalves, M.F.R. Pereira, J.L. Figueiredo, Appl. Catal. A: Gen. 339 (2008) 159.
[28] G. Neri, C. Milone, S. Galvagno, A.P.J. Pijpers, J. Schwank, Appl. Catal. A: Gen. 227 (2002) 105.
[29] S. Galvagno, A. Donato, G. Neri, R. Pietropaolo, G. Capannelli, J. Mol. Catal. 78 (1993) 227.
[30] I.M. Vilella, I. Borbáth, J.L. Margitfalvi, K. Lázár, S.R. de Miguel, O.A. Szelza, Appl. Catal. A: Gen. 326 (2007) 37.
[31] G.C. Torres, S.D. Ledesma, E.L. Jablonski, S.R. de Miguel, O.A. Scelza, Catal. Today 48 (1999) 65.
[32] S.R. de Miguel, M.C. Román-Martínez, E.L. Jablonski, J.L. Fierro, D. Cazorla-Amorós, O.A. Scelza, J. Catal. 184 (1999) 514.
[33] I.M.J. Vilella, S.R. de Miguel, O.A. Scelza, J. Mol. Catal. A: Chem. 284 (2008) 161.
[34] I.M.J. Vilella, S.R. de Miguel, C. Salinas-Martínez de Lecea, A. Linares-Solano, O. Scelza, Appl. Catal. A: Gen. 281 (2005) 247.
[35] F. Coloma, J. Llorca, N. Horms, P. Ramírez de la Piscina, F. Rodríguez-Reinoso, A. Sepúlveda-Escribano, Phys. Chem. Chem. Phys. 2 (2000) 3063.
[36] N. Homs, J. Llorca, P. de la Piscina, F. Rodriguez-Reinoso, A. Sepúlveda-Escribano, J. Silvestre-Albero, Phys. Chem. Chem. Phys. 3 (2001) 1782.
[37] W. Kooamornpattana, J.M. Winterbottom, Catal. Today 66 (2001) 277.
[38] A. Dandekar, R.T.K. Baker, M.A. Vannice, J. Catal. 184 (1999) 421.
[39] J. Court, J. Jablonski, S. Hamar-Thibault, in: M. Guisnet et al. (Eds.), Heterogeneous Catalysis and Fine Chemical III, Elsevier Science Publishers B.V., 1993, p 155.
[40] J.-M. Nhut, L. Pesant, J.-P. Tessonnier, G. Winé, J. Guille, C. Pham-Huu, M.-J. Ledoux, Appl. Catal. A: Gen. 254 (2003) 345.
[41] Q.-H. Yang, P.-X. Hou, S. Bai, M.-Z. Wang, H.-M. Cheng, Chem. Phys. Lett. 345 (2001) 18.
[42] E. Antolini, Appl. Catal. B: Environ. 88 (2009) 1.
[43] J.L. Gómez de la Fuente, M.V. Martínez-Huerta, S. Rojas, P. Terreros, J.L. Fierro, M.A. Peña, Catal. Today 116 (2006) 422.
[44] E. Asedegbega-Nieto, A. Guerrero-Ruiz, I. Rodríguez-Ramos, Carbon 44 (2006) 804.
[45] J.C. Serrano-Ruiz, A. López-Cudero, J. Solla-Gullón, A. Sepúlveda-Escribano, A. Aldaz, F. Rodríguez-Reinoso, J. Catal. 253 (2008) 159.
[46] Y. Li, G.-H. Lai, R.-X. Zhou, Appl. Surf. Sci. 253 (2007) 4978.
[47] R.M. Malek Abbaslou, J. Soltan, A.K. Dalai, Appl. Catal. A: Gen. 379 (2010) 129.
[48] A. Solhy, B.F. Machado, J. Beausoleil, Y. Kihn, F. Goncalves, M.F.R. Pereira, J.J.M. Orfão, J.L. Figueiredo, J.L. Faria, P. Serp, Carbon 46 (2008) 1194.
[49] Z.-T. Liu, C.-X. Wang, Z.-W. Liu, J. Lu, Appl. Catal. A: Gen. 344 (2008) 114.
[50] H. Ma, L. Wang, L. Chen, C. Dong, W. Yu, T. Huang, Y. Qian, Catal. Commun. 8 (2007) 452.
[51] H. Vu, F. Goncalves, R. Philippe, E. Lamouroux, M. Corrias, Y. Kihn, D. Plee, P. Kalck, P. Serp, J. Catal. 240 (2006) 18.
[52] J. Teddy, A. Falqui, A. Corrias, D. Carta, P. Lecante, I. Gerber, P. Serp, J. Catal. 278 (2011) 59.
[53] Z. Guo, Y. Chen, L. Li, X. Wang, G.L. Haller, Y. Yang, J. Catal. 276 (2010) 314.
[54] J.-P. Tessonier, L. Pesant, G. Ehret, M.J. Ledoux, C. Pham-Huu, Appl. Catal. A: Gen. 288 (2005) 203.
[55] P.D. Zgolicz, J.P. Stassi, M.J. Yañez, O.A. Scelza, S.R. de Miguel, J. Catal. 290 (2012) 37.
[56] G. Guo, F. Qin, D. Yang, C. Wang, H. Xu, S. Yang, Chem. Mater. 20 (2008) 2291.
[57] Y.-J. Zhang, J.-Y. Li, W.-Z. Li, Q. Xin, J. Chin. Univ. 26 (2005) 1345.
[58] Y. Tang, D. Yang, F. Qin, J. Hu, C. Wang, H. Xu, J. Solid State Chem. 182 (2009) 2279.
[59] F. Qin, W. Shen, C. Wang, H. Xu, Catal. Commun. 9 (2008) 2095.
[60] J. Khanderi, R.C. Hoffmann, J. Engstler, J.J. Schneider, J. Arras, P. Claus, G. Cherkashinin, Chem. – A Eur. J. 16 (2010) 2300.
[61] J.E. Benson, M. Boudart, J. Catal. 4 (1965) 704.
[62] C.D. Wagner, W.M. Riggs, L.E. Davis, J.F. Moulder, G.E. Muilenberg, Handbook of X-ray Photoelectron Spectroscopy, Perkin-Elmer Co., Physical Electronics, 1979.
[63] J.L. Figueiro, M.F.R. Pereira, M.M.A. Freitas, J.J.M. Órfão, Carbon 37 (1999) 1379.
[64] S.R. de Miguel, O.A. Scelza, M.C. Román-Martínez, C. Salinas-Martínez de Lecea, D. Cazorla-Amarós, A. Linares Solano, Appl. Catal. A: Gen. 170 (1998) 93.
[65] M.C. Román-Martínez, D. Cazorla-Amorós, A. Linares-Solano, C. Salinas-Martínez de Lecea, Carbon 31 (1993) 895.
[66] E. Papirer, S. Li, J.-B. Donnet, Carbon 25 (1987) 243.
[67] A.B. da Silva, E. Jordão, M.J. Mendes, P. Fouilloux, Appl. Catal. A: Gen. 148 (1997) 253.
[68] Y. Li, P.-F. Zhu, R.X. Zhou, Appl. Surf. Sci. 254 (2008) 2609.
[69] A.D. Lueking, R.T. Yang, Appl. Catal. A: Gen. 265 (2004) 259.
[70] A. Huidobro, A. Sepúlveda-Escribano, F. Rodríguez-Reinoso, Stud. Surf. Sci. Catal. 138 (2001) 275.
[71] D.N. Blakely, G.A. Somorjai, J. Catal. 42 (1976) 181.
[72] M. Boudart, Adv. Catal. 20 (1969) 153.
[73] R. Hirschl, F. Delbecq, P. Sautet, J. Hafner, J. Catal. 217 (2003) 354.
[74] R. Hirschl, F. Delbecq, P. Sautet, J. Hafner, Phys. Rev. B 66 (2002) 155438.
[75] F. Delbecq, F. Vigné-Maeder, C. Becker, C. Becker, J. Breitbach, K. Wandelt, J. Phys. Chem. C 112 (2008) 555.
[76] M.T. Paffett, S.C. Gebhard, R.G. Windham, B.E. Koel, J. Phys. Chem. 94 (1990) 6831.
[77] A.K. Shukla, M. Neergat, P. Bera, V. Jayaram, M.S. Hegde, J. Electroanal. Chem. 504 (2001) 111.
[78] N.H. Tran, M.A. Wilson, A.S. Milev, J.R. Bartlett, R.N. Lamb, D. Martin, G.S.K. Kannangara, Adv. Colloid Interface Sci. 145 (2009) 23.
[79] P.C.J. Graat, M.A.J. Somers, Appl. Surf. Sci. 100–101 (1996) 36.
[80] T. Ma, Q. Fu, Y. Cui, Z. Zhang, Z. Wang, D. Tang, X. Bao, Chin. J. Catal. 31 (2010) 24.
[81] P.D. Zgolicz, V.I. Rodríguez, I.M.J. Vilella, S.R. de Miguel, O.A. Scelza, Appl. Catal. A: Gen. 392 (2011) 208.
[82] H.E. van Dam, H. van Bekkum, J. Catal. 131 (1991) 335.
[83] S.A. Bocanegra, A. Guerrero-Ruis, S.R. de Miguel, O.A. Scelza, Appl. Catal. A: Gen. 277 (2004) 11.
[84] E. Janin, M. Björkqvit, T.M. Grehk, M. Göthelid, C.-M. Pradier, U.O. Karlsson, A. Rosengren, Appl. Surf. Sci. 99 (1996) 371.
[85] D.I. Jerdev, A. Olivas, B.E. Koel, J. Catal. 205 (2002) 278.
[86] R.V. Hull, L. Li, Y. Xing, C.C. Chusuei, Chem. Mater. 18 (2006) 1780.
[87] Y. Liu, W. Jiang, L. Xu, X. Yang, F. Li, Mater. Lett. 63 (2009) 2526.
[88] G. Neri, C. Milone, A. Donato, L. Mercadante, A.M. Visco, J. Chem. Technol. Biotechnol. 60 (1994) 83.
[89] M. Burgener, R. Wirz, T. Mallat, A. Baiker, J. Catal. 228 (2004) 152.
[90] U.K. Singh, M.A. Vannice, Appl. Catal. A: Gen. 213 (2001) 1.
[91] B. Moraweck, P. Bondot, D. Goupil, P. Foilloux, A.J. Renouprez, J. Phys. (París) C8 (1987) 48.
[92] P. Beccat, J.C. Bertolini, Y. Gauthier, J. Massadier, P. Ruiz, J. Catal. 126 (1990) 451.
[93] D. Richard, J. Ockelford, A. Giroir-Fendler, P. Gallezot, Catal. Lett. 3 (1989) 53.
[94] F. Delbecq, P. Sautet, J. Catal. 220 (2003) 115.
[95] E. Janin, H. von Schenck, S. Ringler, J. Weissenrieder, T. Akermark, M. Göthelid, J. Catal. 215 (2003) 245.